Inorganic Chemistry

ARTICLE

pubs.acs.org/IC

VO^{2+} Complexation by Bioligands Showing Keto−Enol Tautomerism: A Potentiometric, Spectroscopic, and Computational Study

Daniele Sanna,[†] Katalin Varnágy,[‡] Sarolta Timári,[‡] Giovanni Micera,[§] and Eugenio Garribba*[,§]

[†]Istituto CNR di Chimica Biomolecolare, Trav. La Crucca 3, I-07040 Sassari, Italy

[‡]Department of Inorganic and Analytical Chemistry, University of Debrecen, H-4010 Debrecen, Hungary

[§]Dipartimento di Chimica e Centro Interdisciplinare per lo Sviluppo della Ricerca Biotecnologica e per lo Studio della Biodiversità della Sardegna, Università di Sassari, Via Vienna 2, I-07100 Sassari, Italy

ABSTRACT: The interaction of VO^{2+} ion with ligands of biological interest that are present in important metabolic pathways—2-oxopropanoic acid (pyruvic acid, pyrH), 3-hydroxy-2-oxopropanoic acid (3-hydroxypyruvic acid, hydpyrH), oxobutanedioic acid (oxalacetic acid, $oxalH_2$), (*S*)-hydroxybutanedioic acid (L-malic acid, $malH_2$), and 2,3-dihydroxy-(*E*)-butanedioic acid (dihydroxyfumaric acid, $dhfH_2$)—was described. Their complexing capability was compared with that of similar ligands: 3-hydroxy-2-butanone (hydbut) and 3,4-dihydroxy-3-cyclobutene-1,2-dione (squaric acid, $squarH_2$). All of these ligands (except L-malic acid) exhibit keto−enol tautomerism, and the presence of a metal ion can influence such an equilibrium. The different systems were studied with electron paramagnetic resonance (EPR) and UV−vis spectroscopies and with pH potentiometry. Density functional theory (DFT) methods provide valuable information on the relative energy of the enol and keto forms of the ligands both in the gas phase and in aqueous solution, on the geometry of the complexes, and on EPR and electronic absorption parameters. The results show that most of the ligands behave like α-hydroxycarboxylates, forming mono- and bis-chelated species with (COO^-, O^-) coordination, demonstrating that the metal ion is able to stabilize the enolate form of some ligands. With dihydroxyfumaric acid, the formation of a non-oxidovanadium(IV) complex, because of rearrangement of dihydroxyfumaric to dihydroxymaleic acid ($dhmH_2$), can be observed. With 3-hydroxy-2-butanone and 3,4-dihydroxy-3-cyclobutene-1,2-dione, complexation of VO^{2+} does not take place and the reason for this behavior is explained by chemical considerations and computational calculations.

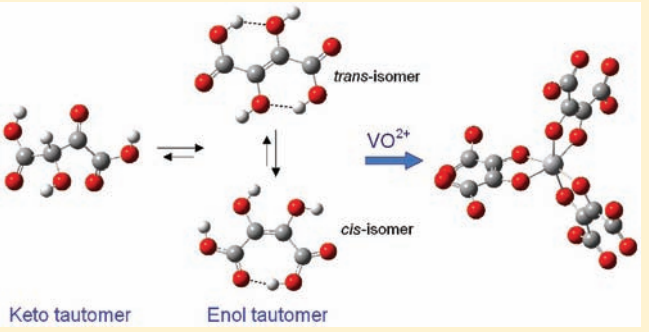

INTRODUCTION

The biological importance of vanadium is well-known.[1] In the higher animals, it plays an essential role even if its biochemical functions have not been fully explained and still remain unclear.[2] Furthermore, vanadium compounds exhibit a wide variety of pharmacological properties, among which are insulin-like effects.[3,4]

About 90% of the vanadium present in the blood is associated with the plasma fraction,[2a] and over the last years, it has been suggested that it is transported in the blood in the oxidation state +IV in the VO^{2+} form, almost independently on the initial state;[2,5,6] if vanadate appears in the blood, it is quickly converted to the VO^{2+} ion in the erythrocytes by glutathione[7] or in the plasma by several reducing bioligands.[8] In vivo blood circulation monitoring−electron paramagnetic resonance (EPR) studies on rats confirm these data,[9] and the binding of VO^{2+} to the bioligands can further stabilize the +IV state and prevent its oxidation to vanadium(V). Therefore, the study of complexation of the VO^{2+} ion by ligands in the biological fluids can give valuable information on the redox processes that vanadium undergoes in the organism and on the form with which it is present in the blood and is transported toward the target organs.

Because V^{IV} is a hard ion, it prefers binding with O donors, mainly if negatively charged, like those provided by carboxylate, alcoholate, phenolate, and phosphate groups. In this work, interaction of the VO^{2+} ion with some important bioligands, such as 2-oxopropanoic acid (pyruvic acid, pyrH), 3-hydroxy-2-oxopropanoic acid (3-hydroxypyruvic acid, hydpyrH), oxobutanedioic acid (oxalacetic acid, $oxalH_2$), (*S*)-hydroxybutanedioic acid (L-malic acid, $malH_2$), and a derivative of fumarate, 2,3-dihydroxy-(*E*)-butanedioic acid (dihydroxyfumaric acid, $dhfH_2$), was studied through the combined application of EPR and UV−vis spectroscopies and pH potentiometry. 3-Hydroxy-2-butanone (hydbut) and 3,4-dihydroxy-3-cyclobutene-1,2-dione (squaric acid, $squarH_2$) were studied for comparison. They are represented in Scheme 1.

As is known, pyruvate is the final product of glycolysis and is formed by dephosphorylation of phosphoenolpyruvate; for each molecule of glucose transformed in the process, two molecules of pyruvic acid are obtained. Moreover, it can also be converted to

Received: June 29, 2011
Published: September 08, 2011

ACS Publications © 2011 American Chemical Society

Scheme 1. Ligands

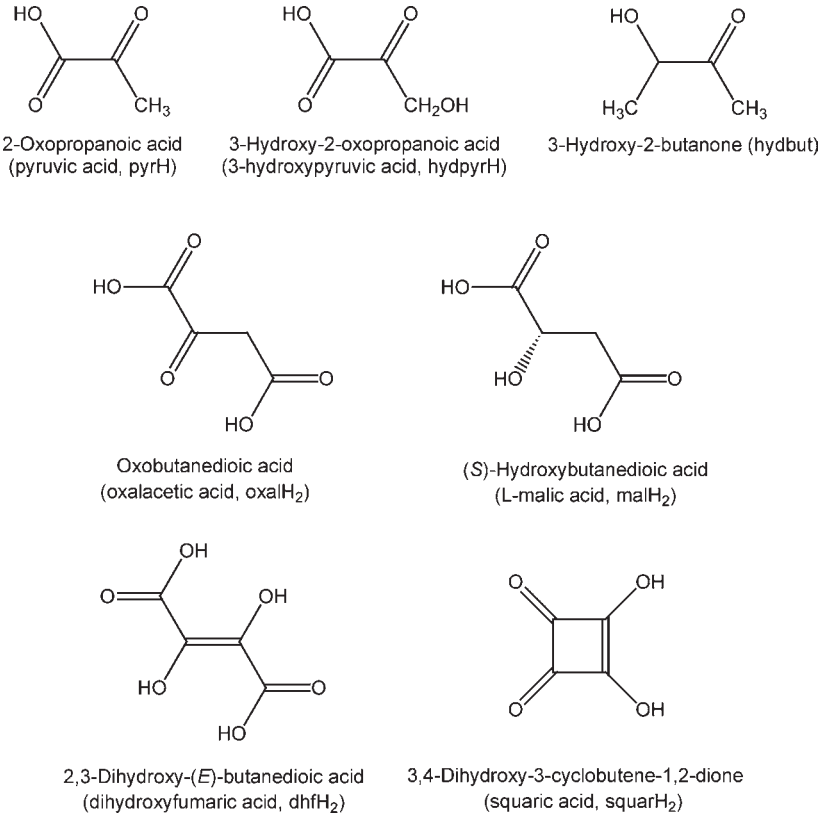

Scheme 2. Keto−Enol Tautomerism

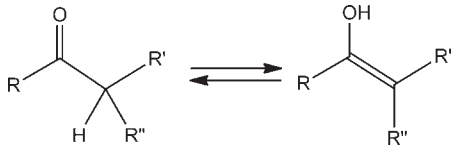

carbohydrates via gluconeogenesis and to fatty acids through acetyl-CoA. On the whole, it has a key role in both the anabolism and catabolism of carbohydrates. Oxalacetate is an intermediate of the citric acid cycle and gluconeogenesis; it is formed in the Krebs cycle upon oxidation of L-malate, catalyzed by malate dehydrogenase, and reacts with acetyl-CoA to form citrate by citrate synthase. L-Malate takes part in the Krebs cycle as the product of hydroxylation of fumarate, catalyzed by fumarase, and is a precursor of oxalacetate. Finally, dihydroxyfumaric acid is a derivative of fumaric acid, which, in turn, is an important product of biochemical reactions: fumarate is formed by oxidation of succinate promoted by succinate dehydrogenase in electron transport chain in mitochondria, where it is subsequently converted to malate by fumarase.

From a chemical point of view, all of the ligands studied (except L-malic acid) show keto−enol tautomerism, illustrated in Scheme 2.

In the literature, it is reported that the relative amount of the enol form at equilibrium is influenced by the solvent and substituents R, R′, and R″. In the case of simple ketones, such an amount is very low; however, it can increase if other keto, aldehyde, ester, or carboxylic groups are present in the molecule. For example, it is reported that, for dihydroxyfumaric and oxalacetic acid, the enol form is more stable,[10−12] while for pyruvic acid and 3-hydroxy-2-butanone, the keto form has the lower energy.[13] Therefore, it can be very interesting to investigate whether V^{IV} is able to stabilize the enol tautomer; indeed, in aqueous solution, the enol can undergo deprotonation of the −OH group (see Scheme 2) to yield enolate, which possesses a greater affinity with respect to the keto tautomer toward a hard metal ion like V^{IV}.

In the present study, EPR and electronic absorption spectroscopy allow very well for distinguishing the coordination mode (COO^-, O^-), similar to hydroxyacids, and (O^-, O^-), characteristic of catechol derivatives, both possible for the enolate form of the studied ligands, from that (COO^-, CO) and (CO, O^-) of the keto tautomer. Therefore, the study of complexation with these bioligands can put in evidence variability in the coordination mode and geometry of vanadium(IV) species and the way with which the VO^{2+} ion interacts with such biomolecules. The experimental results were compared with those obtained from density functional theory (DFT) calculations on the ligands and vanadium(IV) complexes.

EXPERIMENTAL AND COMPUTATIONAL SECTION

Chemicals. Water was deionized prior to use through the purification system Millipore Milli-Q Academic. Sodium pyruvate (Aldrich), 3-hydroxypyruvic acid (Aldrich), 3-hydroxy-2-butanone (Fluka), oxalacetic acid (Fluka), L-malic acid (Fluka), dihydroxyfumaric acid (Aldrich) and 3,4-dihydroxy-3-cyclobutene-1,2-dione (Aldrich) were of the highest

dx.doi.org/10.1021/ic201392d |Inorg. Chem. 2011, 50, 10328–10341

Table 1. pK_a Values of the Ligands and Stability Constants ($\log\beta$) of the VO^{2+} Complexes at 25.0 ± 0.1 °C and I = 0.20 M (KCl)[a]

	$dhfH_2$	$dhmH_2$	pyrH	hydpyrH	$oxalH_2$	$malH_2$	$malH_2$[b]
pK_{a1}	2.91(2)	<1	2.27(1)	2.69(1)	2.43(1)	3.19(1)	3.17
pK_{a2}	4.09(1)	6.68(4)			3.80(1)	4.61(1)	4.47
VOLH							6.9
VOL	6.73(6)		1.87(4)	2.18(3)	2.87(34)	5.19(1)	4.3
VOL_2H_2							13.1
VOL_2H							11.4
VOL_2					6.5[c]	8.31(9)	7.8
$VOLH_{-1}$	2.44(8)		−1.41(2)	−0.58(9)	−0.71(15)	1.08(8)	0.6
$VOLH_{-2}$							−4.4
VOL_2H_{-1}					3.0[c]	4.16(5)	2.8
VOL_2H_{-2}			−4.10(15)	−2.16(3)	−2.16(41)	−1.69(6)	−4.2
VOL_2H_{-3}				−8.22(9)			
VOL_2H_{-4}				−17.80(12)			
VOB_2H_{-2}		3.39(53)					
$VB_3H_{-6}\cdot H_2O$ (VOB_3H_{-4})		−3.35(75)					

[a] The uncertainties (σ values) are given in parentheses. [b] Values are taken from ref 50. [c] Only an approximate value can be given.

grade available and were used as received. VO^{2+} solutions were prepared from $VOSO_4\cdot 3H_2O$ following literature methods.[14]

Potentiometric Measurements. The stability constants of proton and VO^{2+} complexes were determined by pH-potentiometric titrations on 3−4 mL of samples. The ligand to metal molar ratio was between 1:1 and 35:1 and VO^{2+} concentration was 0.0005−0.004 M. Titrations were performed from pH 2.0 until precipitation or very extensive hydrolysis by adding carbonate-free KOH of known concentration (ca. 0.2 M KOH).[15] The pH was measured with a Metrohm 6.0234.110 combined electrode, calibrated for hydrogen ion concentration by the method of Irving et al.[16]

Measurements were carried out at 25.0 ± 0.1 °C and at a constant ionic strength of 0.2 M KCl with a MOLSPIN pH-meter and a MOLACS microburet (0.50 mL) controlled by computer. The use of 0.2 M KCl instead of 0.16 M NaCl (physiological condition) provides the smaller change in the diffusion potential during the pH measurement in the whole pH range than the physiological condition. Purified argon was bubbled through the samples to ensure the absence of oxygen. The number of experimental points was 50−70 for each titration curve and the reproducibility of the points included in the evaluation was within 0.005 pH unit in the measured pH range. In the case of oxalacetic acid the number of experimental points was lower, around 20, because it decomposes in alkaline solution and in the presence of the metal ions; therefore, individual samples were used for determining the stability constants of the VO^{2+} complexes.

The stability of the complexes, reported as the logarithm of the overall formation constant $\beta_{pqr} = [(VO)_pL_qH_r]/[VO]^p[L]^q[H]^r$, where VO stands for VO^{2+} ion, L is the deprotonated form of the ligand and H is the proton, has been calculated with the aid of the SUPERQUAD[17] and PSEQUAD programs.[18] As there were only a few data points in the case of oxalacetic acid, the stability constants of metal−ligand complexes were estimated by the HYPERQUAD program.[19] With the use of this program it was possible to compare the measured titration curve with the one calculated from the stability constants of the complexes. Standard deviations were based on random errors. The conventional notation has been used: negative indices for protons indicate either the dissociation of groups which do not deprotonate in the absence of VO^{2+} coordination, or hydroxido ligands. Hydroxido complexes of VO^{2+} were taken into account and the following species were assumed: $[VO(OH)]^+$ ($\log\beta_{10-1}$= −5.94), $[(VO)_2(OH)_2]^{2+}$ ($\log\beta_{20-2}$ = −6.95), with stability constants calculated from the data of Henry et al.[20] and corrected for the different ionic strengths by use of the Davies equation,[21] $[VO(OH)_3]^-$ ($\log\beta_{10-3}$ = −18.0) and $[(VO)_2(OH)_5]^-$ ($\log\beta_{20-5}$ = −22.0).[22] The uncertainty (σ values) of the stability constants is given in parentheses in Table 1.

Spectroscopic Measurements. Anisotropic EPR spectra were recorded on aqueous solutions with an X-band (9.4 GHz) Bruker EMX spectrometer at 120 K. As usual for low temperature measurements, a few drops of DMSO were added to the samples to ensure good glass formation. The spectra were simulated with the computer program Bruker WinEPR SimFonia,[23] using the highest symmetry molecular axis as z direction; for the VO^{2+} species this coincides with the V═O bond, while for the V^{IV} non-oxido complexes with the axis with the shortest V−O distances. Electronic spectra were recorded with Perkin-Elmer Lambda 35 spectrophotometer in the same concentration range as used for potentiometry. All operations were performed under a purified argon atmosphere in order to avoid oxidation of VO^{2+} ion.

DFT Calculations. All the calculations presented in this paper were performed with DFT methods,[24] and the Gaussian 03 (revision C.02) software.[25] The hybrid exchange-correlation B3LYP,[26,27] and B3P86,[26,28] and the half-and-half BHandHLYP functional, as incorporated in the Gaussian 03, were used.

For keto and enol tautomers, the energy was determined for all the possible conformers by applying the B3LYP functional with 6-311++g(d,p) basis set (indicated also as 6-311++g**) in the gas phase or in water. The solvent has been considered in the polarizable continuum model (PCM) framework.[29] For all the structures, minima were verified through frequency calculations. The relative stability of the two tautomers in the gas phase (g) is the difference between the keto and enol free energies calculated as follows: $\Delta G^{tot}(g) = \Delta E^{ele}(g) + \Delta G^{therm}(g)$, where $\Delta E^{ele}(g)$ is the difference between the electronic plus nuclear repulsion energies and $\Delta G^{therm}(g)$ is the difference between the thermal contributions, estimable using the ideal gas model from the calculated harmonic vibrational frequencies to determine the correction due to zero point energy (ZPE) and to thermal population of the vibrational levels. The relative Gibbs free energy in aqueous solution ($\Delta G^{tot}(aq)$) is the sum of $\Delta E^{ele}(g)$ and $\Delta(\Delta G^{solv}(aq))$, where $\Delta(\Delta G^{solv}(aq))$ is the difference between the solvation free energy of the keto and enol tautomers: $\Delta G^{tot}(aq) = \Delta E^{ele}(g) + \Delta(\Delta G^{solv}(aq))$.

All the geometries of the VO^{2+} complexes investigated were first preoptimized at the B3P86/sto-3g level and further optimized at the level of theory B3P86/6-311g in the gas phase. The optimized structures in the gas phase were used to predict the ^{51}V hyperfine coupling constants (A_{iso}, A_x, A_y and A_z) measurable from EPR spectra. A_{iso}, A_x, A_y

dx.doi.org/10.1021/ic201392d |Inorg. Chem. 2011, 50, 10328–10341

Scheme 3. Equilibrium between Dihydroxyfumaric Acid and Dihydroxymaleic Acid

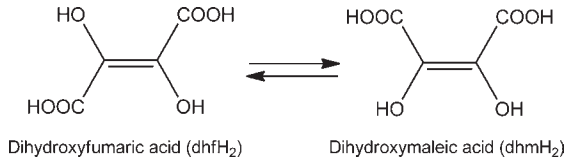

and A_z were simulated at the level of theory BHandHLYP/6-311 g(d,p); $A_{x,y,z}$ were calculated as sum of the isotropic Fermi contact (A^{iso}) and the anisotropic or dipolar hyperfine interaction ($A_{x,y,z} = A^{iso} + A^{D}_{x,y,z}$). The percent deviation from the absolute experimental value, $|A_z|^{exptl}$, was calculated as: $100[(|A_z|^{calcd} - |A_z|^{exptl})/|A_z|^{exptl}]$. The performance of BHandHLYP functional in the calculation of ^{51}V hyperfine coupling constant along the z axis on 22 representative VO^{2+} complexes with different charges, geometries and coordination modes was recently tested, with a mean deviation from $|A_z|^{exptl}$ of 2.7%.[30]

Time-dependent DFT (TD-DFT) calculations,[31] used to predict the excited-states of the VO^{2+} complexes and obtain the expected electronic absorption spectra, were performed at the level of theory B3LYP/6-311g; they were based on the geometry simulated in the gas phase.

RESULTS AND DISCUSSION

1. Studies in Aqueous Solution. *a. VO^{2+}/Dihydroxyfumaric (Dihydroxymaleic) Acid System.* In aqueous solution, dihydroxyfumaric acid is in equilibrium with dihydroxymaleic acid ($dhmH_2$);[11] they differ by the relative positions of the alcoholic and carboxylic substituents: *trans* in the first case and *cis* in the second one (Scheme 3). Such an equilibrium is due to the existence of the keto forms, which allow for interconversion between the two configurational isomers. The crystalline structure of $dhfH_2$ has been reported,[32] but in the literature, it has been pointed out that the *cis* arrangement is slightly more stable than the *trans* one.[10]

The pH-titrations of the free ligand can be fitted by postulating the presence in aqueous solution of a ligand LH_2 with two pK_a values (2.91 and 4.09; see Table 1) and of an "impurity" indicated with BH_2 with only one value of pK_a in the measurable pH range (6.68; Table 1), with the first deprotonation having a pK_a lower than 1. The ratio between of the two forms of the ligands is not constant: it is around 3 in a freshly prepared solution but diminishes during storage of the solution. It can be supposed that LH_2 corresponds to dihydroxyfumaric acid, whereas the other compound is dihydroxymaleic acid, formed as a consequence of isomerization of the ligand. The two pK_a values of the two carboxylic groups of $dhfH_2$ are comparable with those reported in the literature (1.57 and 3.36),[33] whereas pK_a of $dhmH_2$ belongs to one of the two −COOH. The values can be compared with those of fumaric acid (pK_{a1} = 3.02−3.07 and pK_{a2} = 4.39−4.58[34]) and maleic acid (pK_{a1} = 1.92 and pK_{a2} = 6.23[35]). The reason for the larger difference between the pK_a values of dihydroxymaleic acid and maleic acid with respect to dihydroxyfumaric acid and fumaric acid is that, when one proton is removed from the first −COOH of the *cis* isomer ($dhmH_2$ or maleic acid), a strong intramolecular hydrogen bond is formed with the nearby remaining carboxylic group, which hinders removal of the second proton; on the contrary, in the *trans* isomer ($dhfH_2$ or fumaric acid), the two −COOH groups are always far apart, so that hydrogen bonding is not observed and dissociation of the groups is independent from each other.[36]

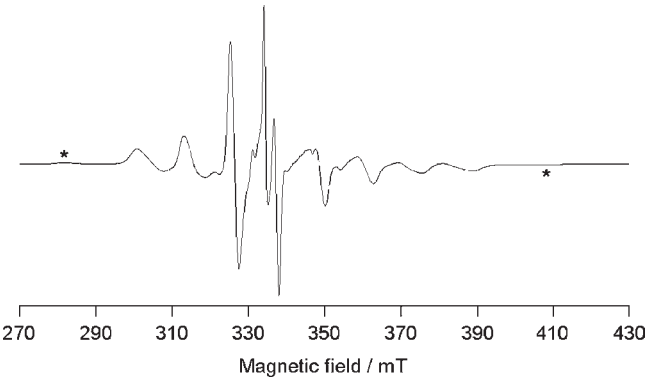

Figure 1. X-band anisotropic spectrum recorded at pH 6.35 on a frozen aqueous solution containing 5 mM VO^{2+} and 50 mM $dhfH_2$. The resonances of a minor VO^{2+} species are denoted with asterisks.

If the complexing capability toward a metal ion is considered, it can be noticed that dihydroxyfumaric acid can use the donor set (COO^-, O^-) to give five- or six-membered chelate rings or to form bridging structures with both the couples (COO^-, O^-), as observed with B^{III}.[37] On the contrary, dihydroxymaleic acid may coordinate a metal ion with the rather strong donor set (O^-, O^-), as reported for the compound bis(tricyclohexylphosphine)-(dimethylmaleate-2,3-diolato-*O*,*O*′)platinum(II).[38]

An examination of the system VO^{2+}/$dhfH_2$ in aqueous solution shows that, even if very low ligand-to-metal ratios are used (5:1), a non-oxidovanadium(IV) complex is formed and that this is the main species in the pH range 5.0−9.0. Small amounts of VO^{2+} complexes, in which presumably carboxylate and/or alkoxide groups bind the metal ion, are observed at lower pH values or coexist with non-oxido species. The formation of hexacoordinated vanadium(IV) complexes depends on the presence of strong donors able to replace the oxido ligand from the VO^{2+} group, for example, the derivatives of catechol.[39] Because in dihydroxyfumaric acid the two −OH groups are in the *trans* position, it is necessary to suppose that, as a matter of fact, the isomer coordinating vanadium(IV) is dihydroxymaleic acid, which can bind vanadium with two deprotonated alcoholic groups on the carbon atoms connected by the double bond, in a hexacoordinated structure that resembles that formed by catechol. Therefore, such a species can be indicated as $[V(dhmH_{-2})_3]^{8-}$ or, if $dhmH_2$ is denoted with BH_2, as $V(BH_{-2})_3$ (see Table 1), where the negative index denotes hydrogen atoms that undergo deprotonation in the presence of the metal ion (in this case, those belonging to −OH) and the electrical charge is due to the alkoxide and carboxylate groups. The EPR spectrum of $[V(dhmH_{-2})_3]^{8-}$ is shown in Figure 1; the spectral parameters are g_x = 1.947, g_y = 1.943, g_z = 1.985 and $A_x = 118 \times 10^{-4}$ cm^{-1}, $A_y = 108 \times 10^{-4}$ cm^{-1}, $A_z \sim 10 \times 10^{-4}$ cm^{-1}.

$[V(dhmH_{-2})_3]^{8-}$ is characterized by $g_x \sim g_y < g_z \sim 2$ and $A_x \sim A_y \gg A_z \sim 0$, values typical for a hexacoordinated vanadium(IV) species with a distorted geometry toward the trigonal prism[40] and significantly different from those of VO^{2+} complexes for which $g_z < g_x \sim g_y < 2$ and $A_z \gg A_x \sim A_y \gg 0$.[41] Therefore, $[V(dhmH_{-2})_3]^{8-}$ can be distinguished very well from VO^{2+} species that are formed by the other ligands and that will be described in the next sections.

dx.doi.org/10.1021/ic201392d |*Inorg. Chem.* 2011, 50, 10328–10341

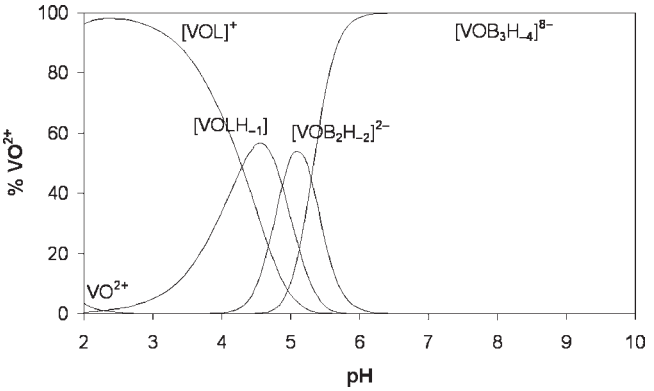

Figure 2. Species distribution diagram for the VO^{2+}/$dhfH_2$ (LH_2)/$dhmH_2$ (BH_2) system as a function of the pH with a molar ratio of 1:4:4 and a VO^{2+} concentration of 2 mM.

The formation of a non-oxidovanadium(IV) species is confirmed by the electronic absorption spectra, which show very intense transitions in the visible region ($\varepsilon > 2500\ M^{-1}\ cm^{-1}$), which give a dark-purple color to the sample, much more intense than those observed in the VO^{2+} complexes ($\varepsilon < 100\ M^{-1}\ cm^{-1}$). The detection of absorption bands between 350 and 750 nm with values of ε in the range of $2000-12\,000\ M^{-1}\ cm^{-1}$ is a distinctive feature of the non-oxidovanadium(IV) species formed by catechol derivatives.[39a,42] Such bands have been interpreted in terms of charge-transfer transitions; in particular, Raymond and co-workers proposed that, for such kinds of metal complexes, these absorptions must be considered ligand-to-metal charge transfers (LMCT) between the a_2 and e_π orbitals of a catechol-like ligand and e_a (d_{xy}, $d_{x^2-y^2}$) and e_b (d_{xz}, d_{yz}) orbitals of vanadium in the D_3 symmetry of the complexes.[42c]

The results of the potentiometric titrations of the binary system VO^{2+}/$dhfH_2$ confirm these assumptions. The distribution curves as a function of the pH are represented in Figure 2 and the stability constants of VO^{2+} complexes in Table 1. As a matter of fact, the data can be interpreted in terms of a ternary system with $dhfH_2$ (LH_2), which binds VO^{2+} mainly in acid solution (pH 2−5), and $dhmH_2$ (BH_2), which coordinates the metal ion at higher pH values (pH >5), forming VOB_2H_{-2} with $2 \times (COO^-, O^-)$ donor sets and the non-oxido species $V(BH_{-2})_3$ (indicated by potentiometry, as usual, as $VB_3H_{-6}\cdot H_2O$ or VOB_3H_{-4}); in this way, dihydroxymaleic acid is subtracted from the equilibrium $dhfH_2 \rightleftharpoons dhmH_2$, allowing the quantitative formation of $V(BH_{-2})_3$.

b. VO^{2+}/3-Hydroxy-2-butanone System. 3-Hydroxy-2-butanone, having a carbonyl group adjacent to an alcoholic carbon atom, could, in principle, give rise to an endiolic structure analogous to that of dihydroxyfumaric acid (Scheme 4), with the possibility of a (O^-, O^-) coordination mode. Nevertheless, in the system VO^{2+}/3-hydroxy-2-butanone, no formation of metal complexes is observed by EPR and potentiometry. DFT results (see below) suggest that, in this case, the equilibrium between the keto and enol tautomers is shifted toward the left with an equilibrium constant in water at 298.15 K of about 4×10^{-7}; for 3-hydroxy-2-butanone, the endiolic form is not stabilized by resonance or through the formation of intramolecular hydrogen bonds and, consequently, has a rather high energy with respect to the keto tautomer.

c. VO^{2+}/3,4-Dihydroxy-3-cyclobutene-1,2-dione (Squaric Acid) System. 3,4-Dihydroxy-3-cyclobutene-1,2-dione or squaric acid has two alcoholic groups on two adjacent carbon atoms connected by a double bond; from a structural point of view, it is similar to dihydroxymaleic acid, which, as previously discussed, coordinates the VO^{2+} ion with formation of non-oxidovanadium(IV) complexes.

Scheme 4. Equilibrium between the Keto (a) and Enol (b) Tautomers of 3-Hydroxy-2-butanone

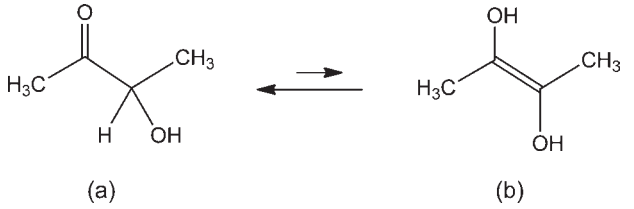

Scheme 5. Comparison between the "Bite" of Dihydroxymaleic Acid (in Red) and Squaric Acid (in Black)

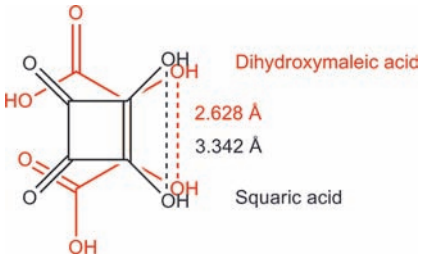

In the literature, two pK_a values are reported for the free ligand (1.70 and 2.89[43]). By potentiometric methods, it is not possible to determine pK_a below 2, and only one value [2.99(1)] is measured, in good agreement with the literature data. However, pH-titrations on the VO^{2+}/$squarH_2$ system are not able to detect any acid−base processes in the measurable pH range. EPR spectra confirm this observation and show that the metal ion undergoes hydrolytic processes at pH higher than 5.

DFT calculations (see below) indicate that the main difference between dihydroxymaleic acid and squaric acid is the ligand "bite", i.e., the distance between the two alcoholic groups that, in the deprotonated form, should bind the VO^{2+} ion. Such a distance is 2.628 Å in the first case and 3.342 Å in the second one (Scheme 5). Therefore, the very large "bite" of squaric acid precludes the formation of stable chelated rings.

d. VO^{2+}/Pyruvic Acid System. Like the ligands illustrated previously, pyruvic acid can exhibit keto−enol tautomerism too (Scheme 6). In the literature, it is reported that the energy difference between the most stable conformers of the enol and keto tautomers is in the range 25−31 kJ/mol in the gas phase and about 14 kJ/mol in water.[13] Therefore, both forms coexist in aqueous solution.

Anisotropic EPR spectra (Figure 3) recorded on frozen solutions containing the VO^{2+} ion and pyruvic acid with metal-to-ligand molar ratios of 1:2 and 1:10 show the formation of two main species with parameters $g_z = 1.942$ and $A_z = 168.2 \times 10^{-4}\ cm^{-1}$ (L:M = 2:1; pH 4.50) and $g_z = 1.956$ and $A_z = 155.5 \times 10^{-4}\ cm^{-1}$ (L:M = 10:1; pH 10.20). A_z values allow one to rule out the (COO^-, CO) coordination of pyruvate because for the "additivity rule" the contribution to A_z of carboxylate and carbonyl groups should result in hyperfine coupling constants of

dx.doi.org/10.1021/ic201392d |Inorg. Chem. 2011, 50, 10328–10341

Scheme 6. Equilibrium between the Keto (a) and Enol (b) Tautomers of Pyruvic Acid

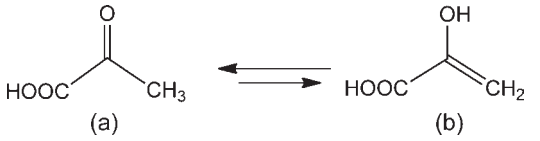

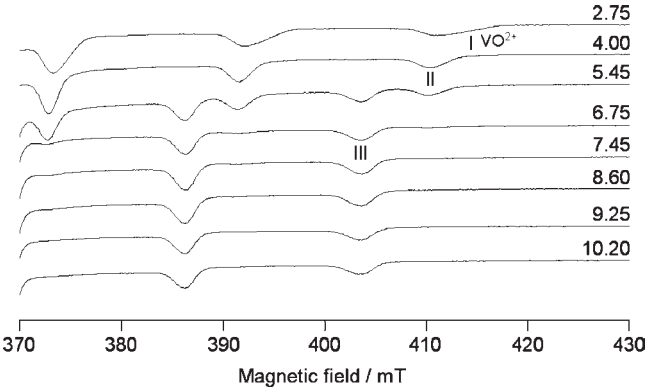

Figure 3. High-field region of the X-band anisotropic EPR spectra recorded as a function of the pH on an aqueous solution of the VO^{2+}/pyrH system with a molar ratio of 1:10 and a VO^{2+} concentration of 5 mM. VO^{2+} and I–III indicate the resonances of $[VO(H_2O)_5]^{2+}$, $[VOL]^+$, $[VOLH_{-1}]$, and $[VOL_2H_{-2}]^{2-}$ complexes, respectively.

176.8×10^{-4} and 171.2×10^{-4} cm^{-1} for mono- and bis-chelated species, respectively.[44,45] The spectroscopic parameters of two complexes, instead, are very similar to those of α-hydroxyacids,[46] indicating that coordination of the metal ion stabilizes the enol tautomer that coordinates the VO^{2+} ion, after deprotonation, in the enolate form with the donor set (COO^-, O^-). Such species can be denoted as $[VOLH_{-1}]$ and $[VOL_2H_{-2}]^{2-}$. pH-potentiometric titrations confirm this interpretation, suggesting the formation of $[VOL]^+$, $[VOLH_{-1}]$, and $[VOL_2H_{-2}]^{2-}$ species (Table 1).

The EPR spectrum of $[VOL_2H_{-2}]^{2-}$ (Figure 4) is rhombic with three g values ($g_z < g_x \neq g_y$) and three A values ($A_z > A_x \neq A_y$).[46] The spectrum was simulated with the following parameters: $g_x = 1.990$, $g_y = 1.981$, $g_z = 1.956$, $A_x = 45.0 \times 10^{-4}$ cm^{-1}, $A_y = 53.5 \times 10^{-4}$ cm^{-1}, and $A_z = 155.5 \times 10^{-4}$ cm^{-1}.

The electronic absorption spectrum of $[VOL_2H_{-2}]^{2-}$ (Figure 5a) shows the presence of four bands in the visible region, suggesting a loss of degeneracy between the d_{xz} and d_{yz} orbitals, due to distortion of the species toward the trigonal bipyramid.[46] This confirms that, in the bis-chelated complex, analogous to α-hydroxycarboxylates, the (COO^-, O^-) donor set binds the VO^{2+} ion. The four absorptions can be simply described in terms of $d_{xy} \rightarrow d_{xz}$, $d_{xy} \rightarrow d_{yz}$, $d_{xy} \rightarrow d_{x^2-y^2}$, and $d_{xy} \rightarrow d_{z^2}$ transitions;[46] their absorption molar coefficient is smaller than 40 M^{-1} cm^{-1}, demonstrating their d–d character.

Therefore, it can be concluded that interaction of the VO^{2+} ion with pyruvic acid stabilizes the enolate form, resulting in a shift toward the right of the pyrH-ket $\rightleftarrows$ pyrH-enol and pyrH-enol $\rightleftarrows$ pyr-enolate equilibria.

e. VO^{2+}/3-Hydroxypyruvic Acid System. With respect to pyruvic acid, 3-hydroxypyruvic shows one more –OH group on the terminal carbon atom (Scheme 7). The presence of such a group

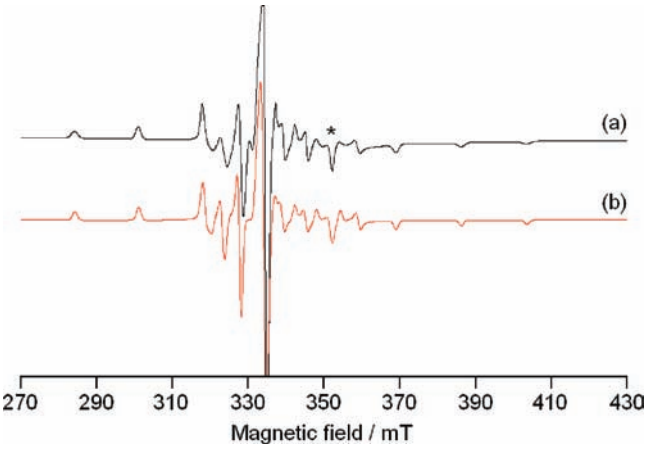

Figure 4. X-band anisotropic EPR spectra recorded at pH 10.20 on an aqueous solution of the VO^{2+}/pyrH system with a molar ratio of 1:10 and a VO^{2+} concentration of 5 mM: (a) experimental; (b) simulated. In the region indicated with an asterisk, the (x,y) anisotropy is observable.

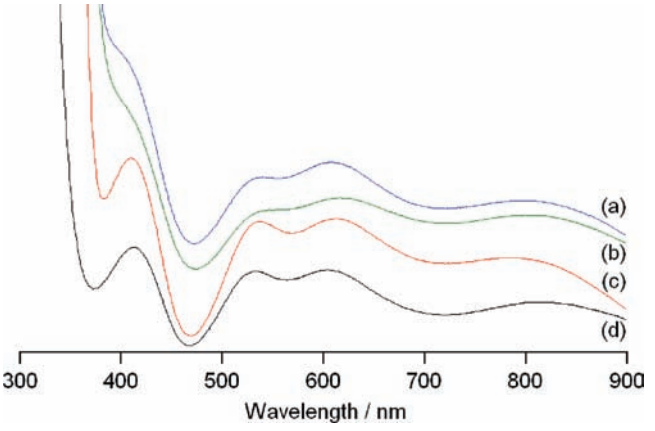

Figure 5. Electronic absorption spectra recorded with a VO^{2+} concentration of 5 mM: (a) pyruvic acid (pH 7.15, L:M = 10); (b) oxalacetic acid (pH 8.60, L:M = 10); (c) 3-hydroxypyruvic acid (pH 7.85, L:M = 10); (d) L-malic acid (pH 9.45, L:M = 35).

Scheme 7. Equilibrium between the Keto (a) and Enol (b) Tautomer of 3-Hydroxypyruvic Acid

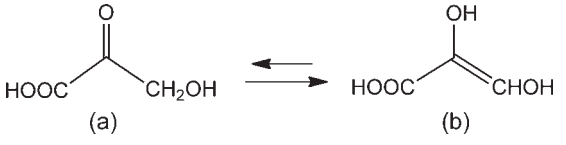

stabilizes the enol form through the formation of intramolecular hydrogen bonds: DFT methods indicate that, while in the gas phase the keto form has lower energy, in an aqueous solution the inversion takes place and the enol tautomer becomes the most stable. This favors complexation of the ligand as hydroxycarboxylate and suggests that formation of non-oxido species similar to those formed by $dhmH_2$ with the couple (O^-, O^-) may be possible around physiological pH. Rather surprisingly, this is not observed, and the ligand at pH 7.4 binds the VO^{2+} ion with the donor set (COO^-, O^-), forming a five-membered chelate ring like α-hydroxycarboxylate.[46]

dx.doi.org/10.1021/ic201392d |*Inorg. Chem.* 2011, 50, 10328–10341

Scheme 8. Equilibrium between the Keto (a) and Enol (b) Forms of Oxalacetic Acid

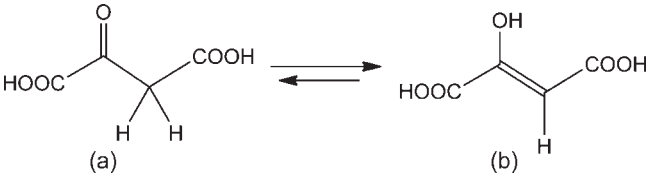

The difference with dihydroxymaleic acid, for which deprotonation of both −OH groups takes place at pH <6, is due to the lack of an electron-withdrawing carboxylic group on one of the terminal carbon atoms, which disfavors deprotonation of the second −OH group at low pH values. Therefore, the stability of the enol tautomer is not the only criterion to be evaluated in order to determine the complexation scheme of this type of ligands.

Potentiometry shows that 3-hydroxypyruvic acid forms VO^{2+} complexes with stoichiometry $[VOL]^{+}$, $[VOLH_{-1}]$, $[VOL_2H_{-2}]^{2-}$, $[VOL_2H_{-3}]^{3-}$, and $[VOL_2H_{-4}]^{4-}$ (Table 1); non-oxidovanadium(IV) species cannot be detected. EPR spectroscopy confirms these insights and suggests that the coordination mode of hydpyrH is typical of simple α-hydroxycarboxylates in the pH range 3−9.[46] In particular, the EPR spectrum of $[VOL_2H_{-2}]^{2-}$ is clearly rhombic ($g_x = 1.982$, $g_y = 1.973$, $g_z = 1.949$, $A_x = 45.0 \times 10^{-4}$ cm^{-1}, $A_y = 53.0 \times 10^{-4}$ cm^{-1}, and $A_z = 156.0 \times 10^{-4}$ cm^{-1}), and the electron absorption spectrum has four bands in the visible region (410, 537, 611, and 782 nm with ε in the range 18−32 M^{-1} cm^{-1}; Figure 5c).

Only at pH >10 does the second −OH group undergo deprotonation, forming $[VOL_2H_{-3}]^{3-}$ and $[VOL_2H_{-4}]^{4-}$. EPR parameters are $g_z = 1.960$ and $A_x = 153.9 \times 10^{-4}$ cm^{-1} in the first case and $g_z = 1.962$ and $A_z = 151.6 \times 10^{-4}$ cm^{-1} in the second one and can be attributed to the (COO^-, O^-); (O^-, O^-), and 2 × (O^-, O^-) coordination modes.[47]

f. VO^{2+}/Oxalacetic Acid System. From a structural point of view, oxalacetic acid is similar to dihydroxyfumaric acid but has only one alcoholic group; because of this difference, it should not form the non-oxidovanadium(IV) complexes previously described (Scheme 8). Analogous to what was reported for pyruvic acid, an equilibrium between the keto and enol tautomers exists, but different from that case, the enol structure seems to be the most stable. Flint and co-workers demonstrated that in aqueous solution and in the solid state the *trans*-enol form mainly exists;[12] this contrasts with what has been recently published by Delchev and Delcheva, who calculated that in the gas phase the keto should be more stable than the enol tautomer of about 54 kJ/mol.[48] In the paragraph on DFT calculations, it will be shown that our data do not agree with this affirmation and are, instead, in agreement with ^{1}H and ^{13}C NMR measurements;[12] in fact, our simulations indicate that the equilibrium constant for keto−enol tautomerism (K_{eq}; Table 2) is approximately 3×10^4; i.e., the enol form is predominant. Concerning the complexing behavior, this results in the possibility of binding the VO^{2+} ion with the couple (COO^-, O^-) of an α-hydroxyacid, with the formation a five-membered chelate ring.

pH-titrations allow one to measure the pK_a of 2.43 and 3.80, attributable to the carboxylic groups. The values are comparable to 2.21 and 3.73 reported in the literature.[49] The distribution curves for the VO^{2+}/oxalH$_2$ system as a function of the pH are shown in Figure 6.

Table 2. Equilibrium Constant (K_{eq}) Calculated by DFT Methods at 298.15 K for the Tautomerization Keto ⇄ Enol

ligand	K_{eq}(gas)	K_{eq}(water)
dihydroxyfumaric acid	∼5×10^8	∼3×10^4
3-hydroxy-2-butanone	∼3×10^{-8}	∼4×10^{-7}
pyruvic acid	∼6×10^{-10}	∼7×10^{-6}
3-hydroxypyruvic acid	∼3×10^{-2}	∼1×10^2
oxalacetic acid	∼2×10	∼3×10^4

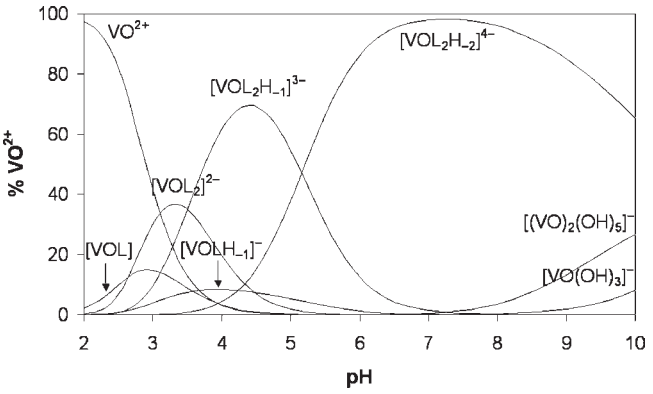

Figure 6. Species distribution diagram for the VO^{2+}/oxalH$_2$ system as a function of the pH with a molar ratio of 1:5 and a VO^{2+} concentration of 2 mM.

The complexation process starts with the formation of minor species [VOL] and $[VOL_2]^{2-}$ around pH 3 (see also Figure 7). The measured EPR parameters of $[VOL_2]^{2-}$, $g_z = 1.956$ and $A_z = 171.5 \times 10^{-4}$ cm^{-1}, are in good agreement with those predicted by the "additivity rule" and DFT methods (see below) for a complex with 2 × (COO^-, CO) coordination. EPR spectra recorded in the pH range 3.0−5.5 show a continuous decrease of the hyperfine coupling constant A_z, which could indicate the presence in aqueous solution of $[VOLH_{-1}]^-$ and $[VOL_2H_{-1}]^{3-}$, with the second species becoming more important with increasing pH. The parameters measured at pH 5.6, $g_z = 1.957$ and $A_z = 163.0 \times 10^{-4}$ cm^{-1}, support a mixed coordination (COO^-, CO); (COO^-, O^-): interestingly, A_z is intermediate between those of the species $[VOL_2]^{2-}$ with 2 × (COO^-, CO) coordination and of $[VOL_2H_{-2}]^{4-}$ with 2 × (COO^-, O^-). $[VOL_2H_{-2}]^{4-}$ predominates in solution above pH 6.0 and is countersigned by $g_z = 1.959$ and $A_z = 155.6 \times 10^{-4}$ cm^{-1}; its electronic absorption spectrum (displayed in Figure 5b) is typical of α-hydroxyacids and shows four bands in the 400−800 nm range, with ε between 16 and 32 M^{-1} cm^{-1}. As for pyruvic acid, the absorption at higher energy is a shoulder of a more intense charge-transfer transition.

Therefore, potentiometric and EPR studies indicate that oxalacetic acid is able to coordinate the VO^{2+} ion as an enolate tautomer, forming $[VOLH_{-1}]^-$ and $[VOL_2H_{-2}]^{4-}$, analogous to those of α-hydroxyacids.[46]

g. VO^{2+}/L-Malic Acid System. L-Malic acid is structurally similar to oxalacetic acid, with an alcoholic group (CHOH) that replaces a carbonyl group (C=O). Its VO^{2+} complexes were previously studied, and the authors attributed the pK_a values of 3.17 and 4.47 of the free ligand to dissociation of the two carboxylic groups; the alcoholic function, in the absence of the

dx.doi.org/10.1021/ic201392d |*Inorg. Chem.* 2011, 50, 10328–10341

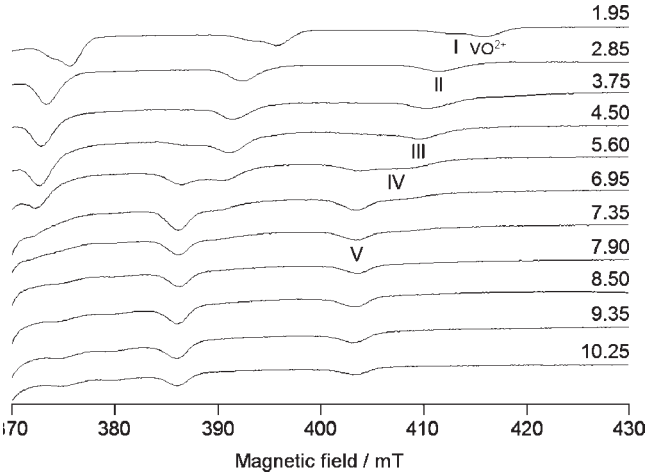

Figure 7. High-field region of the X-band anisotropic EPR spectra recorded as a function of the pH on an aqueous solution of the VO^{2+}/oxalH_2 system with a molar ratio of 1:5 and a VO^{2+} concentration of 5 mM. VO^{2+} and I−V indicate the resonances of $[VO(H_2O)_5]^{2+}$, $[VOL]$, $[VOL_2]^{2-}$, $[VOLH_{-1}]^{-}$, $[VOL_2H_{-1}]^{3-}$, and $[VOL_2H_{-2}]^{4-}$ complexes, respectively.

metal ion, does not undergo deprotonation in the measurable pH range.[50] Our potentiometric studies confirm these data (pK_a = 3.19 and 4.61; Table 1). It is noteworthy that the presence of an oxygen atom on the carbon in the α position to −COOH significantly increases the acidity of the carboxylic group; for example, pK_a goes from 3.96 to 3.19 and 2.43 from succinic acid to malic acid and oxalacetic acid. The acidity increases in the order −H < −OH < =O. For dicarboxylic acids, the presence of such an oxygen also influences deprotonation of the second carboxylic group; in the case of the succinic, malic, and oxalacetic acid series, pK_a decreases from 5.19 to 4.61 and 3.79.

Potentiometric titrations were performed with a very high ligand-to-metal molar ratio, analogous to that reported by Teixeira et al.[50] The presence of a second carboxylic group with respect to a simple α-hydroxyacid disfavors deprotonation of the alcoholic group because of the higher negative charge of the fully deprotonated ligands (L^{3-} instead of L^{2-}).

The composition and stability of the VO^{2+} complexes calculated by pH titrations correspond well to those expected on the basis of EPR measurements. In this case, $[VOL]$ and $[VOL_2]^{2-}$ have (COO^-, OH) and 2 × (COO^-, OH) coordination mode and $[VOLH_{-1}]^{-}$ and $[VOL_2H_{-2}]^{4-}$ (COO^-, O^-) and 2 × (COO^-, O^-), whereas $[VOL_2H_{-1}]^{3-}$ is characterized by a mixed (COO^-, OH); (COO^-, O^-) donor set. From pH 8 to 11, in the existing range of $[VOL_2H_{-2}]^{4-}$ (A_z = 156.5 × 10^{-4} cm^{-1}), another species with a lower ^{51}V hyperfine coupling constant (A_z ∼ 146 × 10^{-4} cm^{-1}) is observed; the intensity ratio between its resonances and those of $[VOL_2H_{-2}]^{4-}$ remains constant with varying pH, suggesting the same stoiochiometry. It has been recently proposed that the presence of an axial donor may decrease the value of A_z,[51] and the results have been recently confirmed.[52] Therefore, it is probable (as confirmed by DFT calculations) that coordination of one carboxylate group belonging to one of the two ligand molecules in the *trans* position to the V=O bond gives a hexacoordinated structure.

An important observation, not reported in the mentioned work,[50] is the presence of four bands in the electronic absorption spectra of the bis-chelated species with 2 × (COO^-, O^-) coordination (Figure 5d), which suggests distortion toward the trigonal bipyramid of the pentacoordinated species, as detected for pyruvic acid, 3-hydroxypyruvic acid, and oxalacetic acid. For L-malate too, the four absorptions fall between 400 and 800 nm and the respective values of the absorption molar coefficient are lower than 30 M^{-1} cm^{-1}. DFT results indicate that the distortion degree is comparable to that observed for the analogous species formed by glycolic acid.

2. DFT Calculations. *a. Stability of the Keto and Enol Tautomers of the Ligands.* As discussed, all of the ligands studied in this work, except L-malic acid, exhibit keto−enol tautomerism. Depending on the relative stability of the two tautomers, coordination to the VO^{2+} ion is possible. Therefore, for each ligand, the free energy in the gas phase and in water at the level of theory B3LYP/6-311++g(d,p) through DFT methods was calculated, with which it is possible to reach a good agreement with the experimental data.[53] The presence of solvent was taken into account within the framework of the PCM.[29] In the absence of the metal ion, the keto/enol group is in the neutral form. Its deprotonation takes place only when the VO^{2+} ion is present in aqueous solutions. Therefore, in the presence of the metal ion, another equilibrium exists, that is, deprotonation of the enol to yield the enolate. For this reason, the results of the calculations on the neutral ligands can be considered as a starting point for the discussion of the data because the possibility that the ligands may coordinate vanadium in the enolate form is connected with the relative stability of the two tautomers in water.

For each tautomer, several conformations were considered; the results for the most stable ones are graphically represented in Scheme 9.

An examination of Scheme 9 allows one to notice that, for dihydroxyfumaric and oxalacetic acid, the enol tautomer is more stable than the keto tautomer. In particular, for dhfH_2, the *cis* isomer (dihydroxymaleic acid) is preferred, both in the gas phase and in water, with respect to the *trans* one: this confirms the results reported in the literature[10] and justifies the complexing behavior of the ligand. For 3-hydroxy-2-butanone and pyruvic acid, the opposite situation is realized and the keto tautomer is favored. For 3-hydroxypyruvic acid, instead, inversion of the stability is predicted and, while the keto form should be slightly more stable in the gas phase, in the aqueous solution, the *cis* and *trans* isomers (almost isoenergetic) of the enol tautomer should be favored.

The stability of several tautomers of dihydroxyfumaric acid is worth discussing. The presence of strong hydrogen bonds and the energy gain due to electronic delocalization explain the higher stability of the two isomers of enol with respect to the keto tautomer. The three most stable conformers are shown in Figure 8. The dotted lines indicate the strongest intramolecular hydrogen bonds that are formed; in water, the H···O distance is 1.535 Å for the *cis* isomer and 1.733 Å for the *trans* one, the O···O distances are 2.529 and 2.574 Å, respectively, while the O−H···O angles are 164.5 and 140.0°. In the most stable conformer of the keto tautomer, not planar, an identical stabilization for resonance does not exist and hydrogen bonds of significant strength are not expected.

Analogous considerations explain the stability order of the tautomers formed by other ligands: a planar and highly delocalized structure and strong hydrogen bonds of 1.756 and 1.812 Å stabilize the enol form of oxalacetic acid and 3-hydroxypyruvic acid, while increasing the shorter H···O distance (2.134 and

Scheme 9. Stability in the Gas Phase and in Water at 298.15 K of (a) Dihydroxyfumaric Acid, (b) 3-Hydroxy-2-butanone, (c) Pyruvic Acid, (d) 3-Hydroxypyruvic Acid, and (e) Oxalacetic Acid[a]

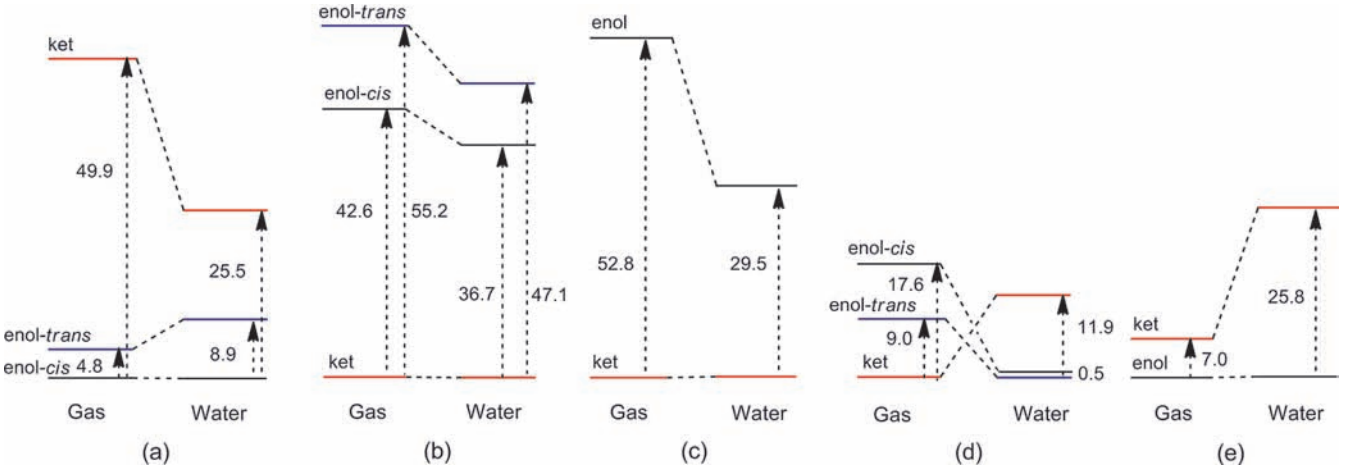

[a] The reported values are in kJ/mol.

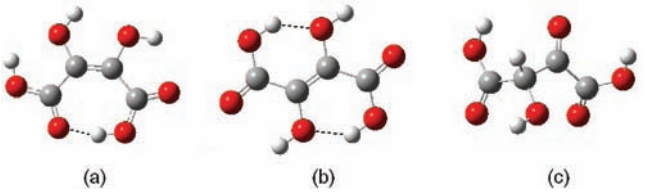

Figure 8. Most stable conformers in water of $dhfH_2$: (a) *cis* isomer of the enol tautomer (dihydroxymaleic acid); (b) *trans* isomer of the enol tautomer (dihydroxyfumaric acid); (c) keto tautomer.

2.171 Å for pyruvic acid and 3-hydroxy-2-butanone, respectively) decreases the stability of enol with respect to the keto tautomer.

An interesting finding emerges from the calculations of the free energy of the deprotonated form of the tautomers in aqueous solution. For example, the difference in the free energy between the enol and keto tautomers of pyruvate decreases by 23.3 kJ/mol with respect to the neutral structures, and this fact and the contemporaneous coordination to the VO^{2+} ion as enolate, which removes the enol form from the keto ⇄ enol equilibrium, favor the tautomerization.

With the free energy data calculated by DFT simulations, it is possible to estimate approximately the value of the equilibrium constant (K_{eq}) for the tautomerization process keto ⇄ enol of several ligands (Table 2). The greater stability of the enol form explains why dihydroxyfumaric acid (in the form of its isomer, dihydroxymaleic acid) coordinates the VO^{2+} ion with the donor set (O^-, O^-), yielding a non-oxido species similar to those formed by catecholates and pyridinonates,[39,54,55] and why pyruvic acid and oxalacetic acid have complexing behavior similar to that of α-hydroxycarboxylates such as glycolate and lactate. 3-Hydroxy-2-butanone, however, does not contain strong anchoring groups in the keto form and is not able to avoid hydrolysis of the VO^{2+} ion.

The behavior of 3-hydroxypyruvic acid deserves a special comment. If the stability in water of the enol tautomer is considered, one may suppose that the formation of a non-oxidovanadium(IV) species similar to that formed by dihydroxymaleic acid could be favored. Instead, the stability of the enol form is a necessary but not sufficient condition to observe the formation of a non-oxido species. The other condition that must be satisfied is deprotonation of the second −OH group, which should take place with a pK_a low enough to allow the oxido ligand to leave as a water molecule: this is possible only if an electron-withdrawing group is present on the carbon atom that brings this alcoholic function. Deprotonation of both of the two −OH groups in dihydroxymaleic acid is favored by the presence of two carboxylates on the two carbon atoms. With 3-hydroxypyruvic acid, the second carbon atom has, instead, one hydrogen atom and the deprotonation step is strongly disfavored and possible only at very basic pH values; this, however, accounts for the (O^-, O^-) coordination at pH >10.

As mentioned above, from the DFT results emerges also the difference in the complexing capability of dihydroxyfumaric acid and 3,4-dihydroxy-3-cyclobutene-1,2-dione, which, in principle, could bind the VO^{2+} ion with the donor set (O^-, O^-). Such a difference can be attributed to the larger "bite" of 3,4-dihydroxy-3-cyclobutene-1,2-dione (see Scheme 5), which precludes the possibility of efficiently chelating the VO^{2+} ion.

b. Optimization of the Structures. The geometry of the non-oxidovanadium(IV) complex formed by dihydroxymaleic acid and that of bis-chelated VO^{2+} species of pyruvic acid, 3-hydroxypyruvic acid, oxalacetic acid, and L-malic acid were optimized through DFT calculations with Gaussian 03 software.[25] Over the last years, it has been demonstrated that the use of such methods of simulation gives good results in the optimization of the structures formed by transition metals;[56] in particular, it has been demonstrated that, for complexes of the first-row transition-metal elements, the order of efficiency of the functionals in terms of mean deviation from the experimental values and corresponding standard deviation is B3P86 ∼ B3PW91 ∼ PBE0 > TPSSh > PBE ∼ B3LYP ∼ TPSS ∼ BPW91 ∼ BP86 > VSXC > BLYP.[56d] Therefore, in this work the functional B3P86, composed of the exchange Becke hybrid (B3)[26] and correlation part P86,[28] was used; it allows one to obtain an excellent agreement with the experimental structures for many vanadium compounds.[56d,57] Regarding the basis sets, a wide possibility of choices exists, even if it seems that they influence the results less than the functional; recently, we found that the valence triple-ζ basis set

dx.doi.org/10.1021/ic201392d |*Inorg. Chem.* 2011, 50, 10328–10341

Table 3. Structural Parameters Calculated for Vanadium(IV) and VO^{2+} Complexes[a]

complex	V=O	V−O^-_{alk}	V−O^-_{carb}	O^-_{alk}−V−O^-_{alk}	O^-_{carb}−V−O^-_{carb}	Φ/τ [b]
$[V(dhmH_{-2})_3]^{8-}$		1.929−1.950		162.3−162.9 [c]		35.1
$[V(cat)_3]^{2-}$ [d]		1.922−1.971		162.1−164.0 [c]		∼39
$[VO(pyrH_{-1})_2]^{2-}$	1.606	1.963	2.007	139.3	149.9	0.15
$[VO(hydpyrH_{-1})_2]^{2-}$	1.607	1.963	2.014	138.2	150.3	0.05
$[VO(oxalH_{-1})_2]^{4-}$	1.614	1.983	2.001	143.9	147.3	0.06
$[VO(oxal)_2]^{2-}$ [e]	1.584	2.047 [f,g]	1.955 [f]	150.3 [h]	129.5	0.09
$[VO(malH_{-1})_2]^{4-}$	1.631	1.925 [f]	2.057 [f]	134.5	156.9	0.37
$[VO(glycH_{-1})_2]^{2-}$	1.617	1.920	2.048	132.0	155.4	0.39
$[VO(benzH_{-1})_2]^{2-}$ [i]	1.584	1.916 [f]	1.971	132.9	151.6	0.31

[a] Distances in Å and angles in deg. [b] Φ and τ are the twist angle and trigonality index, as defined in the text. [c] Angles between the donors are in the *trans* position. [d] Experimental values were taken from ref 39a; for catechol, the donors are phenolate oxygen atoms. [e] (O_{ket}, O^-_{carb}) coordination. [f] Mean distance. [g] V−O_{ket} distance. [h] O_{ket}−V−O_{ket} angle. [i] Experimental values were taken from ref 61.

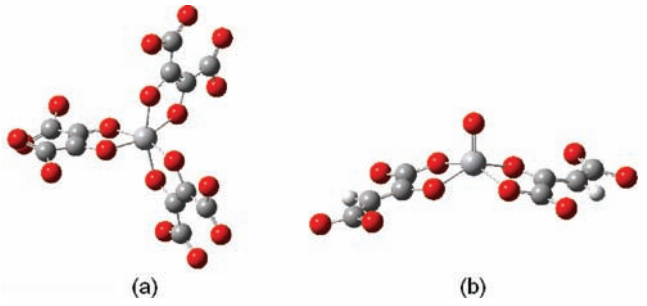

Figure 9. Structure of the complexes $[V(dhmH_{-2})_3]^{8-}$ (a) and $[VO(oxalH_{-1})_2]^{4-}$ (b), optimized by DFT methods in the gas phase at the level of theory B3P86/6-311g.

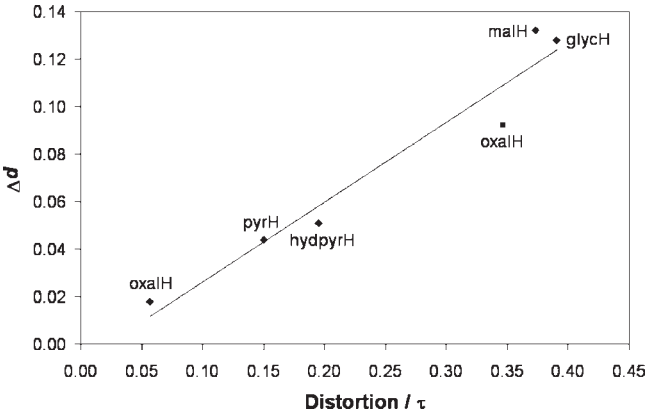

Figure 10. Distortion toward the trigonal bipyramid for $[VO(pyrH_{-1})_2]^{2-}$, $[VO(hydpyrH_{-1})_2]^{2-}$, $[VO(oxalH_{-1})_2]^{4-}$, $[VO(oxal)_2]^{2-}$ (square), $[VO(malH_{-1})_2]^{4-}$ and $[VO(glycH_{-1})_2]^{2-}$ as a function of Δ*d*, where $\Delta d = [d^{mean}(V\text{-}L^{ax}) - d^{mean}(V\text{-}L^{eq})]$ (see the text).

6-311g, developed by Pople and co-workers,[58] is enough to simulate correctly an experimental structure and represents a reasonable compromise between the accuracy and speed of the simulation.[57]

The results are shown in Table 3, where the data for $[VO(oxal)_2]^{2-}$ with 2 × (COO^-, CO) coordination and for $[VO(glycH_{-1})_2]^{2-}$, used as a comparison (glycH = glycolic acid), are included. In Figure 9, the optimized structures of $[V(dhmH_{-2})_3]^{8-}$ and $[VO(oxalH_{-1})_2]^{4-}$ are represented.

The structural data for $[V(dhmH_{-2})_3]^{8-}$ can be compared with those of $[V(cat)_3]^{2-}$,[39a] where H_2cat is catechol (which coordinates vanadium in a similar way with respect to dihydroxymaleic acid with six deprotonated phenolate oxygen atoms): for $[V(cat)_3]^{2-}$, the bond distances V−O^- are in the range 1.922−1.971 Å and the angles between the donors in the *trans* position in the range 162.1−164.0°, in excellent agreement with what was found for $[V(dhmH_{-2})_3]^{8-}$ with DFT simulations.

A hexacoordinated structure of vanadium(IV) can be described both as an octahedron and as a trigonal prism: in the first case, the two equilateral triangles of the polyhedron are rotated with a twist angle (Φ) of 60°, while in the second one, they are perfectly eclipsed with a Φ value of 0°. The value of the twist angle allows one to describe the distortion of the structure with respect to the two limit forms; in most cases, the geometry of a vanadium(IV) species is closer to the trigonal prism than to the octahedron with an experimental value of Φ much smaller than 60°.

An analysis performed by Kepert showed that the stereochemistry for tris(bidentate) complexes $[M(L\text{-}L)_3]$ depends on the ligand−ligand repulsion energy.[59] A critical parameter is the "normalized bite" of the bidentate ligand (*b*), namely, the ratio of the distance between the two donor atoms of the chelated ring to the metal−ligand bond length. For bites of 1.414, the minimum value of the energy, corresponding to the most stable stereochemistry, occurs for the regular octahedron at Φ = 60°, while as the bite is decreased to 1.3−1.2, the upper triangular face is brought into a more eclipsed configuration relative to the other face and the minimum energy moves to lower values of Φ. For $[V(dhmH_{-2})_3]^{8-}$ and $[V(cat)_3]^{2-}$, *b* is 1.26 and 1.29, respectively, and a twist angle much lower than 60° is expected, in agreement with what was calculated; as a comparison, for the compound $[V(S_2P(OEt)_2)_3]$, for which *b* is a bit larger (1.31), the measured value of Φ is slightly greater (41.4°).[60]

Concerning the VO^{2+} species, the simulated data can be compared with those of the only structure formed by α-hydroxycarboxylate for which the X-ray diffractometric analysis exists, the bis-chelated complex of benzilic acid (benzH).[61] For $[VO(benzH_{-1})_2]^{2-}$, the mean lengths of the V−O^-_{alk} and V−O^-_{carb} bonds are 1.916 and 1.971 Å, respectively, and the O^-_{alk}−V−O^-_{alk} and O^-_{carb}V−O^-_{carb} angles are 151.6 and 132.9° (Table 3), similar to the optimized structure of L-malic acid; moreover, a significant distortion of the square pyramid toward the trigonal bipyramid is reported, which can be expressed by the trigonality index τ, defined as $(\beta - \alpha)/60$, where

dx.doi.org/10.1021/ic201392d |*Inorg. Chem.* 2011, 50, 10328–10341

Table 4. ^{51}V Hyperfine Coupling Constants Calculated for V^{IV} and VO^{2+} Complexes.[a]

complex	A_{iso}^{calcd}	T_x^{calcd}	T_y^{calcd}	T_z^{calcd}	A_x^{calcd}	A_y^{calcd}	A_z^{calcd}	$A_z^{exptl\,b}$	% $\lvert A_z\rvert^c$
$[V(dhmH_{-2})_3]^{8-}$	−59.4	−37.7	−25.0	62.8	−97.1	−84.4	3.4	−118.0	−17.7
$[VO(pyrH_{-1})_2]^{2-}$	−79.6	29.1	40.6	−69.7	−50.5	−39.0	−149.3	−155.5	−4.0
$[VO(hydpyrH_{-1})_2]^{2-}$	−80.0	29.1	40.5	−69.6	−50.5	−39.5	−149.6	−156.0	−4.1
$[VO(oxalH_{-1})_2]^{4-}$	−71.3	27.9	41.5	−69.3	−43.4	−29.9	−140.7	−155.6	−9.6
$[VO(oxal)_2]^{2-d}$	−94.8	30.1	34.3	−69.4	−64.7	−60.5	−164.2	−171.5	−4.3
$[VO(malH_{-1})_2]^{4-}$	−71.7	27.7	41.3	−69.0	−44.0	−30.5	−140.7	−156.5	−10.1
$[VO(malH_{-1})_2]^{4-e}$	−65.4	25.7	42.2	−67.9	−39.7	−23.2	−133.3	∼146	−8.7
$[VO(glycH_{-1})_2]^{2-}$	−78.1	29.9	39.6	−69.6	−48.1	−38.4	−147.6	−157.2	−6.1

[a] All of the values were measured in 10^{-4} cm^{-1}. [b] A_x^{exptl} for $[V(dhmH_{-2})_3]^{8-}$. [c] Percentage deviation from the experimental value calculated as $(\lvert A_z\rvert^{calcd} - \lvert A_z\rvert^{exptl})/\lvert A_z\rvert^{exptl}$. [d] 2 × ($COO^-$, CO) coordination mode. [e] (COO^-, O^-, COO^{-ax}); (COO^-, O^-) coordination mode.

β and α are the two angles formed by the two axial and equatorial donors: 1 for trigonal bipyramidal geometry and 0 for square-pyramidal geometry.[62] As pointed out recently in the literature, the distortion toward the trigonal bipyramid increases with the difference between the axial and equatorial bonds, which can be expressed by the formula $\Delta d = [d^{mean}(V\text{-}L^{ax}) - d^{mean}(V\text{-}L^{eq})]$, where d^{mean} indicates the calculated mean distance.[63] When the value of the distortion τ is reported as a function of Δd for the six complexes in Table 3, the expected linear plot is found (Figure 10). Therefore, it can be supposed that all of the VO^{2+} complexes formed by derivatives of α-hydroxycarboxylates follow the same trend.

c. Calculation of the EPR Parameters. As is known, ^{51}V hyperfine coupling constants can be measured from EPR spectra.[41,44,64] In particular, the hyperfine coupling constant along the z axis (A_z) allows for identification of the equatorial donors of a VO^{2+} species through application of the "additivity rule".[44,64] Many articles have been recently published on the possibility of predicting the ^{51}V hyperfine coupling constants in the EPR spectra of VO^{2+} species.[30,65−67] A DFT method for calculating the $\boldsymbol{A}$ tensor has been incorporated in Gaussian 03, which, however, does not include relativistic effects or a spin−orbit contribution. The best overall agreement with experimental A values can be obtained with the non-relativistic method and half-and-half hybrid functional.[30,67b] The performance of half-and-half hybrid functional is connected to the best prediction of the Fermi contact term (A_{iso} for Gaussian software) than to the other methods, which, in turn, depends on the indirect core-level spin polarization arising from the unpaired spin density in the metal d orbitals; the spin polarization is difficult to calculate to high accuracy, and most DFT calculations significantly underestimate it. It has been recently demonstrated that DFT simulations at the BHandHLYP/6-311g(d,p) level of theory allow one to obtain deviations from the experimental value lower than 5% and, in most of cases, 3%.[30] Therefore, nowadays it is possible to predict the value of A_z for an unknown VO^{2+} structure with a good degree of accuracy.

The results of the simulations performed on the complexes $[V(dhmH_{-2})_3]^{8-}$, $[VO(pyrH_{-1})_2]^{4-}$, $[VO(hydpyrH_{-1})_2]^{2-}$, $[VO(oxalH_{-1})_2]^{4-}$, $[VO(oxal)_2]^{2-}$, $[VO(malH_{-1})_2]^{4-}$, and, as a comparison, $[VO(glycH_{-1})_2]^{2-}$ are shown in Table 4.

It can be observed that DFT methods predict correctly the different behavior of the non-oxidovanadium(IV) species $[V(dhmH_{-2})_3]^{8-}$ and oxido VO^{2+} complexes. As reported in Table 4, for $[V(dhmH_{-2})_3]^{8-}$, the order $\lvert A_x\rvert > \lvert A_y\rvert \gg \lvert A_z\rvert$, with $\lvert A_z\rvert$ very small, is expected; this is in agreement with the experimental values (see above). However, the level of theory applied does not return with good accuracy the $\boldsymbol{A}$ tensor for a non-oxidovanadium(IV) complex; probably, this can be related with the different electronic structures with respect to a VO^{2+} species. Concerning the other compounds in Table 4, the A_z value for $[VO(pyrH_{-1})_2]^{2-}$ (and for $[VO(glycH_{-1})_2]^{2-}$) agrees well with that experimentally observed, while for $[VO(oxalH_{-1})_2]^{4-}$ and $[VO(malH_{-1})_2]^{4-}$, a consistent deviation from $\lvert A_z\rvert^{exptl}$ exists (−9.6 and −10.1%, respectively). It has been noticed that DFT methods give very good results with neutral complexes:[30] therefore, the deviation for most of the VO^{2+} species in Table 4 may be attributed to their high negative charges. It is probable that such a charge perturbs the spin-polarization mechanism of the core electrons, which results in a worse prediction of the A_{iso} term.

The simulations predict, in agreement with the experimental data, that, for complexes of the VO^{2+} ion with the 2 × (COO^-, O^-) donor set, the symmetry reduction with respect to C_{4v}, as a consequence of the trigonal bipyramidal distortion, results in a rhombic spectrum with three A ($A_z > A_x \neq A_y$) values.[46,68] For the complexes discussed in this work, however, it is not possible to relate the trigonal bipyramidal distortion with the absolute value of $\lvert A_x - A_y\rvert$, which for simple α-hydroxycarboxylates increases with increasing τ.[46]

DFT calculations suggest also that the species that is present in solution in the system VO^{2+}/L-malic acid, together with the bis-chelated complex with coordination 2 × (COO^-, O^-), may be an isomer in which another carboxylate group of one of the two L-malate ligands occupies the axial position. As demonstrated recently,[51,52] this axial interaction should reduce the value of $\lvert A_z\rvert$ (Table 4).

d. Calculation of the Electronic Absorption Spectra. After recent implementations, TD-DFT methods are nowadays frequently used in the calculation of the electronic transitions of metal complexes.[31,66,69] Such methods describe a given transition in terms of a linear combination of vertical excitations from occupied to virtual molecular orbitals and, consequently, only the dominant character of each transition can be specified. TD-DFT also provides the electric dipole oscillator strength (f) of the transition from the ground state to the excited state, which is related to the transition moment. Up to today, they provide only a qualitative agreement between experimental and calculated spectra; however, the results can be useful in the assignment of the transitions and in the description of the electronic structure of a metal complex.

The most important orbital transitions and their character, the excitation wavelengths and the oscillator strengths calculated at the B3LYP/6-311g level for $[V(dhmH_{-2})_3]^{8-}$,

Table 5. Main Calculated and Experimental Electronic Transitions for V^{IV} and VO^{2+} Complexes

	main transition	character	λ^a	f^b	$\lambda^{exptl\,a,c}/\varepsilon^{exptl\,d}$
$[V(dhmH_{-2})_3]^{8-}$	H−3 → L	$d_{xz/yz} \rightarrow d_{xy}$	1340.7	0.0001	
	H−3 → L+1	$d_{xz/yz} \rightarrow d_{x^2-y^2}$	1286.5	0.0001	
	H → L+1	L → $d_{yz/xz}$	688.1	0.0178	670/2520
	H → L+2	L → L	644.8	0.0091	
	H−2 → L+1	L → $d_{yz/xz}$	597.8	0.0132	
	H → L+3	L → L	590.8	0.0106	
	H−2 → L	L → d_{xy}	552.8	0.0137	520/2730
	H → L+2	L → L	473.5	0.0373	
	H → L+1	L → $d_{yz/xz}$	443.5	0.0436	
	H−2 → L+3	L → L	419.2	0.0237	
	H−1 → L+2	L → L	404.4	0.0440	
	H → L+3	L → L	392.0	0.0190	
$[VO(pyrH_{-1})_2]^{2-}$	H → L+2	$d_{xy} \rightarrow d_{xz}$	678.7	0.0004	795/16
	H → L+3	$d_{xy} \rightarrow d_{yz}$	587.4	0.0009	607/22
	H → L+4	$d_{xy} \rightarrow d_{x^2-y^2}$	510.7	0.0001	538/20
	H → L/H → L+5	$d_{xy} \rightarrow L/d_{xy} \rightarrow d_{z^2}$	430.5	0.0004	400^{sh}/37
$[VO(hydpyrH_{-1})_2]^{2-}$	H → L+4	$d_{xy} \rightarrow d_{xz}$	686.8	0.0005	782/18
	H → L+5	$d_{xy} \rightarrow d_{yz}$	576.5	0.0009	611/23
	H → L+6	$d_{xy} \rightarrow d_{x^2-y^2}$	519.2	0.0001	537/23
	H → L+2/H → L+8	$d_{xy} \rightarrow L/d_{xy} \rightarrow d_{z^2}$	415.0	0.0005	410/32
$[VO(oxalH_{-1})_2]^{4-}$	H → L+2	$d_{xy} \rightarrow d_{xz}$	726.3	0.0003	800/16
	H → L+3	$d_{xy} \rightarrow d_{yz}$	642.5	0.0018	616/18
	H → L+5	$d_{xy} \rightarrow d_{x^2-y^2}$	516.2	0.0001	547/16
	H → L/H → L+6	$d_{xy} \rightarrow L/d_{xy} \rightarrow d_{z^2}$	450.7	0.0004	402^{sh}/32
$[VO(malH_{-1})_2]^{4-}$	H → L	$d_{xy} \rightarrow d_{xz}$	872.1	0.0006	817/14
	H → L+1	$d_{xy} \rightarrow d_{yz}$	573.2	0.0006	604/19
	H → L+4	$d_{xy} \rightarrow d_{x^2-y^2}$	532.5	0.0001	535/19
	H → L +6/H → L+3	$d_{xy} \rightarrow d_{z^2}/d_{xy} \rightarrow L$	412.5	0.0006	412/22
$[VO(glycH_{-1})_2]^{2-}$	H → L	$d_{xy} \rightarrow d_{xz}$	769.2	0.0005	804/22
	H → L+2	$d_{xy} \rightarrow d_{yz}$	528.2	0.0008	606/27
	H → L+6	$d_{xy} \rightarrow d_{x^2-y^2}$	521.6	0.0001	532/28
	H → L +7/H → L+3	$d_{xy} \rightarrow d_{z^2}/d_{xy} \rightarrow L$	389.8	0.0004	405/35

[a] Values measured in nm. [b] Oscillator strength. [c] sh indicates that the band is a shoulder of a most intense absorption. [d] Values measured in M^{-1} cm^{-1}.

$[VO(pyrH_{-1})_2]^{2-}$, $[VO(hydpyrH_{-1})_2]^{2-}$, $[VO(oxalH_{-1})_2]^{4-}$, $[VO(malH_{-1})_2]^{4-}$, and, as a reference compound, for $[VO(glycH_{-1})_2]^{2-}$ are reported in Table 5, where the calculated values are compared with the experimental ones.

TD-DFT simulations suggest for $[VO(pyrH_{-1})_2]^{2-}$, $[VO(hydpyrH_{-1})_2]^{2-}$, $[VO(oxalH_{-1})_2]^{4-}$, $[VO(malH_{-1})_2]^{4-}$, and $[VO(glycH_{-1})_2]^{2-}$ four absorption bands in the range of 390−820 nm, as displayed by the VO^{2+} complexes with a significant distortion toward the trigonal bipyramid, like those formed by α-hydroxycarboxylates.[46] The energy order of the transitions is $d_{xy} \rightarrow d_{xz} < d_{xy} \rightarrow d_{yz} < d_{xy} \rightarrow d_{x^2-y^2} < d_{xy} \rightarrow d_{z^2}$, in agreement with what is reported in the literature.[46] However, it must be remembered that the absorption bands are composite and the high mixing of excited configurations due to the low symmetry of the complexes does not allow one to classify the calculated transitions as pure ligand-field d−d transitions; for example, to the band at 769.2 nm for $[VO(glycH_{-1})_2]^{2-}$ contribute the excitations $d_{xy} \rightarrow d_{xz}$ (HOMO → LUMO) for 65.2%, $d_{xy} \rightarrow$ L (HOMO → LUMO+4) for 15.8%, L → d_{xz} (HOMO−4 → LUMO) for 10.1%, and finally L → d_{xz} (HOMO−3 → LUMO) for 8.9%. From the results, it emerges that the first three absorptions are mainly d−d bands, whereas the last one is mixed with other excitations; in particular, $d_{xy} \rightarrow d_{z^2}$ is mixed with a $d_{xy} \rightarrow$ L excitation (a metal-to-ligand or MLCT transition). The oscillator strengths, which can be related with the absorption molar coefficient ε, are in the range 0.0001−0.0018.

For $[V(dhmH_{-2})_3]^{8-}$, the behavior is completely different: the two transitions between 400 and 800 nm arise from the contribution of a large number of excitations. Different from the spectra of the VO^{2+} complexes examined previously, characterized by d−d absorptions, its spectrum is dominated by intraligand (LL) and ligand-to-metal (LMCT) transitions. This confirms what is suggested by Raymond and co-workers for such species: that all of the transitions have to be considered LMCT, in which the metal orbitals involved are d_{xy}, $d_{x^2-y^2}$, d_{xz}, and d_{yz} (see Table 5).[42c] As a proof of this, the oscillator strength arrives at 0.0178 for the first band and at 0.0440 for the second band. On the whole, these values are about 2 orders of magnitude greater than those of $[VO(pyrH_{-1})_2]^{2-}$, $[VO(hydpyrH_{-1})_2]^{2-}$, $[VO(oxalH_{-1})_2]^{4-}$, $[VO(malH_{-1})_2]^{4-}$, and $[VO(glycH_{-1})_2]^{2-}$. For $[V(dhmH_{-2})_3]^{8-}$, the d−d excitations are expected above 1200 nm and the corresponding oscillator strength is 100−400 times smaller than that of the other bands.

dx.doi.org/10.1021/ic201392d |Inorg. Chem. 2011, 50, 10328–10341

CONCLUSIONS

Interaction of the VO^{2+} ion with important bioligands, such as pyruvic acid, 3-hydroxypyruvic acid, oxalacetic acid, and L-malic acid, and a derivative of fumaric acid, dihydroxyfumaric acid, was examined. 3-Hydroxy-2-butanone and squaric acid were studied as a comparison. For all of the ligands studied (except L-malic acid), the keto and enol tautomers are in equilibrium. DFT calculations show that the position of such an equilibrium depends on the physical state of the ligand, gas phase or aqueous solution, and on the possibility of forming intramolecular hydrogen bonds.

The coordinating strength of the enolate form is greater than the keto one; in fact, in the presence of the VO^{2+} ion, the −OH group easily undergoes deprotonation and the ligands can bind the metal as enolates with the donor set (COO^-, O^-), analogous to that of α-hydroxycarboxylates. The complexing process shifts the position of the equilibria keto ⇄ enol and enol ⇄ enolate toward the right. Therefore, the presence of a metal ion in aqueous solution can significantly influence the keto−enol tautomerism even in the physiological conditions.

The ligands can be divided into three classes. (i) Pyruvic acid, 3-hydroxypyruvic acid, and oxalacetic acid form with VO^{2+} mono- and bis-chelated species with the couple (COO^-, O^-), even when the enol form is strongly disfavored in aqueous solution with respect to the keto one, like in the case of pyruvic acid; the bis-complexes are distorted toward the trigonal bipyramid and are characterized by rhombic EPR and electronic absorption spectra with four d−d bands. (ii) Dihydroxyfumaric acid forms non-oxidovanadium(IV) complexes (i.e., hexacoordinated species without V=O bonds) comparable for structure and spectroscopic behavior to those formed by catechol and its derivatives, implying the presence of the very strong donor set (O^-, O^-); because in dihydroxyfumaric acid the two −OH groups are in the *trans* position and cannot bind simultaneously the metal ion, it is necessary to advance the hypothesis that the *cis* isomer (dihydroxymaleic acid) coordinates the V^{IV} ion; in this case too, the coordination of dihydroxymaleate to vanadium shifts the position of the equilibrium *trans* isomer ⇄ *cis* isomer toward the right and the non-oxido species can be formed quantitatively. However, the presence of two −OH groups on two neighboring carbon atoms in the enol form, like in the case of 3-hydroxypyruvic acid, is a necessary but not sufficient condition to observe the formation of a non-oxido complex, with the other condition being the possibility of deprotonation of the two −OH groups with a sufficiently low p*K*, which is favored by the presence of electron-withdrawing groups, such as −COOH. (iii) Finally, 3-hydroxy-2-butanone and squaric acid, which, in principle, may bind vanadium in the enolate form with (COO^-, O^-) and (O^-, O^-) donor sets, respectively, do not form stable complexes; in the first case, this is due to the greater stability of the keto than the enol tautomer and, in the second one, to the structural features of the ligand.

DFT methods were revealed to be very powerful in predicting the relative stability of the keto and enol forms, both in the gas phase and in an aqueous solution, the structures of VO^{2+} and vanadium(IV) complexes, and their EPR and UV−vis parameters.

AUTHOR INFORMATION

Corresponding Author

*E-mail: garribba@uniss.it.

ACKNOWLEDGMENT

This work was supported by the Hungarian Scientific Research Fund (K 72956) and Gedeon Richter Plc.

REFERENCES

(1) (a) Crans, D. C.; Smee, J. J.; Gaidamauskas, E.; Yang, L. *Chem. Rev.* **2004**, *104*, 849–902. (b) Rehder, D. *Bioinorganic Vanadium Chemistry*; Wiley: Chichester, U.K., 2008.

(2) (a) Nielsen, F. H. In *Metal Ions in Biological Systems*; Sigel, A., Sigel, H., Eds.; Marcel Dekker: New York, 1995; Vol. 31, pp 543−573. (b) Nielsen, F. H. In *Vanadium Compounds: Chemistry, Biochemistry, and Therapeutic Applications*; Tracey, A. S., Crans, D. C., Eds.; ACS Symposium Series 711; American Chemical Society: Washington DC, 1998; pp 297−315.

(3) Costa Pessoa, J.; Tomaz, I.*Curr. Med. Chem.* **2010**, *17*, 3701−3738 and references cited therein.

(4) (a) Shechter, Y.; Karlish, S. J. D. *Nature* **1980**, *284*, 556–558. (b) Thompson, K. H.; McNeill, J. H.; Orvig, C. *Chem. Rev.* **1999**, *99*, 2561−2571 and references cited therein. (c) Thompson, K. H.; Orvig, C. *Coord. Chem. Rev.* **2001**, *219*−*221*, 1033−1053 and references cited therein. (d) Shechter, Y.; Goldwaser, I.; Mironchik, M.; Fridkin, M.; Gefel, D. *Coord. Chem. Rev.* **2003**, *237*, 3–11. (e) Sakurai, H.; Yoshikawa, Y.; Yasui, H. *Chem. Soc. Rev.* **2008**, *37*, 2383–2392.

(5) Kustin, K.; Robinson, W. E. In *Metal Ions in Biological Systems*; Sigel, A., Sigel, H., Eds.; Marcel Dekker: New York, 1995; Vol. 31, pp 511−542.

(6) Kiss, T.; Jakusch, T.; Hollender, D.; Dörnyei, A.; Enyedy, E. A.; Costa Pessoa, J.; Sakurai, H.; Sanz-Medel, A. *Coord. Chem. Rev.* **2008**, *252*, 1153−1162 and references cited therein.

(7) (a) Macara, I. G.; Kustin, K.; Cantley, L. C., Jr. *Biochem. Biophys. Acta* **1980**, *629*, 95–106. (b) Hansen, T. V.; Aaseth, J.; Alexander, J. *Arch. Toxicol.* **1982**, *50*, 195–202.

(8) (a) Kustin, K.; Toppen, D. L. *Inorg. Chem.* **1973**, *12*, 1404–1407. (b) Cantley, L. C., Jr.; Ferguson, J. H.; Kustin, K. *J. Am. Chem. Soc.* **1978**, *100*, 5210–5212. (c) Sakurai, H.; Shimomura, S.; Ishizu, K. *Inorg. Chim. Acta* **1978**, *55*, L67–L69.

(9) Yasui, H.; Takechi, K.; Sakurai, H. *J. Inorg. Biochem.* **2000**, *78*, 185–196.

(10) (a) Hartree, E. F. *J. Am. Chem. Soc.* **1953**, *75*, 6244–6249. (b) Liebman, J. F.; Slayden, S. W. In *The Chemistry of Metal Enolates*; Zabicky, J., Ed.; John Wiley & Sons: Chichester, U.K., 2009; pp 185−221.

(11) Garcia, B.; Ruiz, R.; Leal, J. M. *J. Phys. Chem. A* **2008**, *112*, 4921–4928.

(12) Flint, D. H.; Nudelman, A.; Calabrese, J. C.; Gottlieb, H. E. *J. Org. Chem.* **1992**, *57*, 7270–7274.

(13) (a) Raczyńska, E. D.; Duczmal, K.; Darowska, M. *Vib. Spectrosc.* **2005**, *39*, 37–45. (b) Kakkar, R.; Pathak, M.; Radhika, N. P. *Org. Biomol. Chem.* **2006**, *4*, 886–895. (c) Kakkar, R.; Pathak, M.; Gahlot, P. *J. Phys. Org. Chem.* **2008**, *21*, 23–29.

(14) Nagypál, I.; Fábián, I. *Inorg. Chim. Acta* **1982**, *61*, 109–113.

(15) Gran, G. *Acta Chem. Scand.* **1950**, *4*, 559–577.

(16) Irving, H.; Miles, M. G.; Pettit, L. D. *Anal. Chim. Acta* **1967**, *38*, 475–488.

(17) Gans, P.; Vacca, A.; Sabatini, A. *J. Chem. Soc., Dalton Trans.* **1985**, 1195–1200.

(18) Zékány, L.; Nagypál, I. In *Computation Methods for the Determination of Formation Constants*; Leggett, D. J., Ed.; Plenum Press: New York, 1985; pp 291−353.

(19) Gans, P.; Sabatini, A.; Vacca, A. *Talanta* **1996**, *43*, 1739–1753.

(20) Henry, R. P.; Mitchell, P. C. H.; Prue, J. E. *J. Chem. Soc., Dalton Trans.* **1973**, 1156–1159.

(21) Davies, C. W. *J. Chem. Soc.* **1938**, 2093–2098.

(22) (a) Komura, A.; Hayashi, M.; Imanaga, H. *Bull. Chem. Soc. Jpn.* **1977**, *50*, 2927–2931. (b) Vilas Boas, L. F.; Costa Pessoa, J. In *Comprehensive Coordination Chemistry*; Wilkinson, G., Gillard, R. D., McCleverty, J. A., Eds.; Pergamon Press: Oxford, 1987; Vol. 3, pp 453−583.

(23) *WINEPR SimFonia*, version 1.25; Bruker Analytische Messtechnik GmbH: Karlsruhe, Germany, 1996.
(24) Parr, R. G.; Yang, W. *Density-Functional Theory of Atoms and Molecules*; Oxford University Press: Oxford, U.K., 1989.
(25) Frisch, M. J.; Trucks, G. W.; Schlegel, H. B.; Scuseria, G. E.; Robb, M. A.; Cheeseman, J. R.; Montgomery, J. A., Jr.; Vreven, T.; Kudin, K. N.; Burant, J. C.; Millam, J. M.; Iyengar, S. S.; Tomasi, J.; Barone, V.; Mennucci, B.; Cossi, M.; Scalmani, G.; Rega, N.; Petersson, G. A.; Nakatsuji, H.; Hada, M.; Ehara, M.; Toyota, K.; Fukuda, R.; Hasegawa, J.; Ishida, M.; Nakajima, T.; Honda, Y.; Kitao, O.; Nakai, H.; Klene, M.; Li, X.; Knox, J. E.; Hratchian, H. P.; Cross, J. B.; Adamo, C.; Jaramillo, J.; Gomperts, R.; Stratmann, R. E.; Yazyev, O.; Austin, A. J.; Cammi, R.; Pomelli, C.; Ochterski, J. W.; Ayala, P. Y.; Morokuma, K.; Voth, G. A.; Salvador, P.; Dannenberg, J. J.; Zakrzewski, V. G.; Dapprich, S.; Daniels, A. D.; Strain, M. C.; Farkas, O.; Malick, D. K.; Rabuck, A. D.; Raghavachari, K.; Foresman, J. B.; Ortiz, J. V.; Cui, Q.; Baboul, A. G.; Clifford, S.; Cioslowski, J.; Stefanov, B. B.; Liu, G.; Liashenko, A.; Piskorz, P.; Komaromi, I.; Martin, R. L.; Fox, D. J.; Keith, T.; Al-Laham, M. A.; Peng, C. Y.; Nanayakkara, A.; Challacombe, M.; Gill, P. M. W.; Johnson, B.; Chen, W.; Wong, M. W.; Gonzalez, C.; Pople, J. A. *Gaussian03*, revision C.02; Gaussian, Inc.: Wallingford, CT, 2004.
(26) Becke, A. D. *J. Chem. Phys.* **1993**, *98*, 5648–5652.
(27) Lee, C.; Yang, W.; Parr, R. G. *Phys. Rev. B* **1988**, *37*, 785–789.
(28) (a) Perdew, J. P. *Phys. Rev. B* **1986**, *33*, 8822–8824. (b) Perdew, J. P. *Phys. Rev. B* **1986**, *34*, 7406.
(29) (a) Miertus, S.; Scrocco, E.; Tomasi, J. *Chem. Phys.* **1981**, *55*, 117–129. (b) Miertus, S.; Tomasi, J. *Chem. Phys.* **1982**, *65*, 239–245. (c) Cossi, M.; Barone, V.; Cammi, R.; Tomasi, J. *Chem. Phys. Lett.* **1996**, *255*, 327–335.
(30) Micera, G.; Garribba, E. *Dalton Trans.* **2009**, 1914–1918.
(31) (a) Runge, E.; Gross, E. K. U. *Phys. Rev. Lett.* **1984**, *52*, 997–1000. (b) Casida, M. K. In *Recent Advances in Density Functional Methods*; Chong, D. P., Ed.; World Scientific, Singapore, 1995; Vol. 1, pp 155−192.
(32) Gupta, M. P.; Gupta, N. P. *Acta Crystallogr., Sect. B* **1968**, *24*, 631–636.
(33) Hay, R. W.; Harvie, S. J. *Aust. J. Chem.* **1965**, *18*, 1197–1209.
(34) Venkatnarayana, G.; Swarny, S.; Lingaiah, P. *Indian J. Chem., Sect. A* **1984**, *23A*, 501–503. (b) Cape, J.; Cook, D.; Williams, D. *J. Chem. Soc., Dalton Trans.* **1974**, 1849–1852.
(35) Dissociation Constants of Organic Acids and Bases. In *CRC Handbook of Chemistry and Physics*, Internet version 2005; Lide, D. R., Ed.; CRC Press: Boca Raton, FL, 2005; http://www.hbcpnetbase.com.
(36) Pine, S. H.; Hendrickson, J. B.; Cram, D. J.; Hammond, G. S. *Organic Chemistry*; McGraw-Hill: New York, 1980; section 6-2, ISBN 0070501157.
(37) Yalpani, M.; Boese, R.; Blaser, D. *Chem. Ber.* **1983**, *116*, 3338–3346.
(38) Goel, A. B.; Goel, S. *Angew. Chem., Int. Ed.* **1984**, *23*, 375–376.
(39) (a) Cooper, S. R.; Koh, Y. B.; Raymond, K. N. *J. Am. Chem. Soc.* **1982**, *104*, 5092–5102. (b) Branca, M.; Micera, G.; Dessì, A.; Sanna, D.; Raymond, K. N. *Inorg. Chem.* **1990**, *29*, 1586–1589. (c) Jezowska-Bojczuk, M.; Koslowski, H.; Zubor, A.; Kiss, T.; Branca, M.; Micera, G.; Dessì, A. *J. Chem. Soc., Dalton Trans.* **1990**, 2903–2907. (d) Buglyó, P.; Dessì, A.; Kiss, T.; Micera, G.; Sanna, D. *J. Chem. Soc., Dalton Trans.* **1993**, 2057–2063.
(40) Desideri, A.; Raynor, J. B.; Diamantis, A. A. *J. Chem. Soc., Dalton Trans.* **1978**, 423–426.
(41) Garner, C. D.; Collison, D.; Mabbs, F. E. In *Metal Ions in Biological Systems*; Sigel, A., Sigel, H., Eds.; Marcel Dekker: New York, 1995; Vol. 31, pp 617−670.
(42) (a) Hawkins, C. J.; Kabanos, T. A. *Inorg. Chem.* **1989**, *28*, 1084–1087. (b) Klich, P. R.; Daniher, A. T.; Challen, P. R.; McConville, D. B.; Youngs, W. J. *Inorg. Chem.* **1996**, *35*, 347–356. (c) Karpishin, T. B.; Dewey, T. M.; Raymond, K. N. *J. Am. Chem. Soc.* **1993**, *115*, 1842–1851.
(43) Alexandersson, D.; Vannerberg, N. *Acta Chem. Scand.* **1973**, *27*, 3499–3512.
(44) Chasteen, N. D. In *Biological Magnetic Resonance*; Berliner, L. J., Reuben, J. J., Eds.; Plenum Press: New York, 1981; Vol. 3, pp 53−119.
(45) (a) Hamstra, B. J.; Houseman, A. P. L.; Colpas, G. J.; Kampf, J. W.; LoBrutto, R.; Frasch, W. D.; Pecoraro, V. L. *Inorg. Chem.* **1997**, *36*, 4866–4874. (b) Jakusch, T.; Buglyó, P.; Tomaz, A. I.; Costa Pessoa, J.; Kiss, T. *Inorg. Chim. Acta* **2002**, *339*, 119–128.
(46) Garribba, E.; Micera, G.; Panzanelli, A.; Sanna, D. *Inorg. Chem.* **2003**, *42*, 3981–3987.
(47) Garribba, E.; Lodyga-Chruscinska, E.; Sanna, D.; Micera, G. *Inorg. Chim. Acta* **2001**, *322*, 87−98 and references cited therein.
(48) Delchev, V. B.; Delcheva, G. T. *J. Struct. Chem.* **2007**, *48*, 615–622.
(49) Raghavan, N. G.; Leussing, D. L. *J. Am. Chem. Soc.* **1976**, *98*, 723–730.
(50) Teixeira, M. H. S. F.; Costa Pessoa, J.; Vilas Boas, L. F. *Polyhedron* **1992**, *11*, 697–708.
(51) Gorelsky, S.; Micera, G.; Garribba, E. *Chem.—Eur. J.* **2010**, *16*, 8167–8180.
(52) Mukherjee, T.; Costa Pessoa, J.; Kumar, A.; Sarkar, A. R. *Inorg. Chem.* **2011**, *50*, 4349–4361.
(53) Alagona, G.; Ghio, C. *Int. J. Quantum Chem.* **2008**, *108*, 1840–1855.
(54) Rangel, M.; Leite, A.; Amorim, M. J.; Garribba, E.; Micera, G.; Lodyga-Chruscinska, E. *Inorg. Chem.* **2006**, *45*, 8086–8097.
(55) Buglyò, P.; Kiss, E.; Kiss, T.; Sanna, D.; Garribba, E.; Micera, G. *J. Chem. Soc., Dalton Trans.* **2002**, 2275–2282.
(56) (a) Bühl, M.; Kabrede, H. *J. Chem. Theory Comput.* **2006**, *2*, 1282–1290. (b) Waller, M. P.; Bühl, M. *J. Comput. Chem.* **2007**, *28*, 1531–1537. (c) Waller, M. P.; Braun, H.; Hojdis, N.; Bühl, M. *J. Chem. Theory Comput.* **2007**, *3*, 2234–2242. (d) Bühl, M.; Reimann, C.; Pantazis, D. A.; Bredow, T.; Neese, F. *J. Chem. Theory Comput.* **2008**, *4*, 1449–1459.
(57) Garribba, E.; Micera, G.; Sanna, D. *6th International Symposium on Vanadium Chemistry*, Lisbon, 2008; Book of Abstracts O30.
(58) Krishnan, R.; Binkley, J. S.; Seeger, R.; Pople, J. A. *J. Chem. Phys.* **1980**, *72*, 650–654.
(59) Kepert, D. L. *Inorg. Chem.* **1972**, *11*, 1561–1563.
(60) Furlani, C.; Tomlinson, A. A. G.; Porta, P.; Sgamellotti, A. *J. Chem. Soc. A* **1970**, 2929–2934.
(61) Chasteen, N. D.; Belford, R. L.; Paul, I. C. *Inorg. Chem.* **1969**, *8*, 408–418.
(62) Addison, A. W.; Rao, T. N.; Reedijk, J.; van Rijn, J.; Verschoor, G. C. *J. Chem. Soc., Dalton Trans.* **1984**, 1349–1356.
(63) Lodyga-Chruscinska, E.; Sanna, D.; Garribba, E.; Micera, G. *Dalton Trans.* **2008**, 4903–4916.
(64) Smith, T. S., II; LoBrutto, R.; Pecoraro, V. L. *Coord. Chem. Rev.* **2002**, *228*, 1–18.
(65) *Calculation of NMR and EPR Parameters. Theory and Applications*; Kaupp, M., Bühl, M., Malkin, V. G., Eds.; Wiley-VCH: Weinheim, Germany, 2004.
(66) Neese, F. *Coord. Chem. Rev.* **2009**, *253*, 526−563 and references cited therein.
(67) (a) Munzarová, M. L.; Kaupp, M. *J. Phys. Chem. B* **2001**, *105*, 12644−12652 and references cited therein. (b) Saladino, A. C.; Larsen, S. C. *J. Phys. Chem. A* **2003**, *107*, 1872–1878. (c) Neese, F. *J. Chem. Phys.* **2003**, *118*, 3939–3948. (d) Remenyi, C.; Reviakine, R.; Arbuznikov, A. V.; Vaara, J.; Kaupp, M. *J. Phys. Chem. A* **2004**, *108*, 5026−5033 and references cited therein. (e) Aznar, C. P.; Deligiannakis, Y.; Tolis, E. J.; Kabanos, T.; Brynda, M.; Britt, R. D. *J. Phys. Chem. A* **2004**, *108*, 4310–4321. (f) Saladino, A. C.; Larsen, S. C. *Catal. Today* **2005**, *105*, 122−133 and references cited therein.
(68) Cornman, C. R.; Geisre-Bush, K. M.; Rowley, S. R.; Boyle, P. D. *Inorg. Chem.* **1997**, *36*, 6401–6408.
(69) Rosa, A.; Ricciardi, G.; Gritsenko, O.; Berends, E. J. *Struct. Bonding (Berlin)* **2004**, *112*, 49–115.